

**RESEARCH ARTICLE**

# Full and partial agonists evoke distinct structural changes in opening the muscle acetylcholine receptor channel

 Nuriya Mukhtasimova<sup>1</sup> and Steven M. Sine<sup>1,2,3</sup> 

The muscle acetylcholine (ACh) receptor transduces a chemical into an electrical signal, but the efficiency of transduction, or efficacy, depends on the particular agonist. It is often presumed that full and partial agonists elicit the same structural changes after occupancy of their binding sites but with differing speed and efficiency. In this study, we tested the alternative hypothesis that full and partial agonists elicit distinct structural changes. To probe structural changes, we substituted cysteines for pairs of residues that are juxtaposed in the three-dimensional structure and recorded agonist-elicited single-channel currents before and after the addition of an oxidizing reagent. The results revealed multiple cysteine pairs for which agonist-elicited channel opening changes after oxidative cross-linking. Moreover, we found that the identity of the agonist determined whether cross-linking affects channel opening. For the  $\alpha$ D97C/ $\alpha$ Y127C pair at the principal face of the subunit, cross-linking markedly suppressed channel opening by full but not partial agonists. Conversely, for the  $\alpha$ D97C/ $\alpha$ K125C pair, cross-linking impaired channel opening by the weak agonist choline but not other full or partial agonists. For the  $\alpha$ T51C/ $\alpha$ K125C pair, cross-linking enhanced channel opening by the full agonist ACh but not other full or partial agonists. At the complementary face of the subunit, cross-linking between pairs within the same  $\beta$  hairpin suppressed channel opening by ACh, whereas cross-linking between pairs from adjacent  $\beta$  hairpins was without effect for all agonists. In each case, the effects of cross-linking were reversed after addition of a reducing reagent, and receptors with single cysteine substitutions remained unaltered after addition of either oxidizing or reducing reagents. These findings show that, in the course of opening the receptor channel, different agonists elicit distinct structural changes.

## Introduction

Efficacy, a core principle in receptor pharmacology, is a measure of the relative efficiency, and often the speed, with which occupancy by an agonist activates its receptor (Colquhoun, 1998). For the acetylcholine (ACh) receptor (AChR) from vertebrate skeletal muscle, occupancy by a full agonist opens the receptor channel efficiently and rapidly, whereas occupancy by a partial agonist opens the channel less efficiently and more slowly (Liu and Dilger, 1991, 1993; Maconochie and Steinbach, 1998). Kinetic analyses of agonist-elicited single-channel currents have provided estimates of rate constants governing elementary reaction steps for agonists with differing efficacy. The emerging consensus is that agonists across the efficacy spectrum differ in the rate and extent with which they form a closed state intermediate in the path toward channel opening (Lape et al., 2008, 2009; Mukhtasimova et al., 2009, 2016). In particular, the agonist–receptor complex

transitions from the resting to an intermediate closed state, and then the intermediate state transitions to the open state. The speed and efficiency of forming the intermediate state increase with increasing agonist efficacy, whereas the speed and efficiency of channel opening is agonist independent.

From the standpoint of receptor structure, it is often tacitly presumed that different agonists elicit the same structural changes, but with differing efficiency, speed, or both (Grosman et al., 2000; Lape et al., 2008; Mukhtasimova et al., 2016). However, we recently found that a mutation within the binding–gating transduction pathway attenuated channel opening by a full agonist, whereas it enhanced channel opening by a partial agonist (Mukhtasimova and Sine, 2013). Thus, the functional consequences of the mutation depended on the particular agonist, suggesting agonists with different efficacy transduce binding into

<sup>1</sup>Receptor Biology Laboratory, Department of Physiology and Biomedical Engineering, Mayo Clinic College of Medicine, Rochester, MN; <sup>2</sup>Department of Molecular Pharmacology and Experimental Therapeutics, Mayo Clinic College of Medicine, Rochester, MN; <sup>3</sup>Department of Neurology, Mayo Clinic College of Medicine, Rochester, MN.

Correspondence to Steven M. Sine: [sine@mayo.edu](mailto:sine@mayo.edu).

© 2018 Sine and Mukhtasimova This article is distributed under the terms of an Attribution–Noncommercial–Share Alike–No Mirror Sites license for the first six months after the publication date (see <http://www.rupress.org/terms/>). After six months it is available under a Creative Commons License (Attribution–Noncommercial–Share Alike 4.0 International license, as described at <https://creativecommons.org/licenses/by-nc-sa/4.0/>).

channel gating via distinct structural changes. Such differences might be expected. Different agonists, owing to their different sizes and chemistry, could bind in different poses, or the agonist–receptor interactions could vary in strength, consequently eliciting different downstream structural changes in the course of transduction.

Site-directed mutagenesis is a valuable means to identify residues essential for receptor function, but it provides limited information on structural changes that underpin function. To gain insight into structural changes that transduce agonist binding into channel opening, we substituted cysteine for pairs of residues that come into close proximity in the 3-D structure. We then recorded single-channel currents, before and after addition of oxidizing reagent, elicited by several agonists with diverging efficacy. The results reveal structural regions in which oxidative cross-linking alters channel opening by full but not partial agonists, and conversely, regions in which cross-linking alters channel opening by partial but not full agonists.

## Materials and methods

### Expression of wild-type and mutant AChRs

cDNAs encoding the human  $\alpha$ ,  $\beta$ ,  $\epsilon$ , and  $\delta$  subunits, installed within the cytomegalovirus expression vector pRBG4 (Lee et al., 1991), were transfected into BOSC 23 cells (Pear et al., 1993). Cysteine substitutions were generated by using the QuikChange site-directed mutagenesis kit (Agilent Technologies); the presence of the cysteine substitutions and the absence of unintended mutations were confirmed by sequencing the coding region. Cells were maintained in Dulbecco's modified Eagle's medium containing 10% (vol/vol) FBS at 37°C until they reached ~50% confluence. Thereafter, cDNAs encoding wild-type or mutant AChR subunits, plus a cDNA-encoding GFP, were transfected by calcium-phosphate precipitation. Patch-clamp recordings were made 12–48 h after transfection. For each receptor with double cysteine substitutions, recordings were obtained from three to eight independent transfections.

### Single-channel recordings

Patch-clamp recordings were obtained in the cell-attached patch configuration with a membrane potential of  $-70$  mV and a temperature of 21°C. The pipette solution contained (in mM) 80 KF, 20 KCl, 40 potassium aspartate, 2 MgCl<sub>2</sub>, 1 EGTA, and 10 HEPES, adjusted to pH 7.4 with KOH; this calcium-free pipette solution was chosen because it facilitated formation of gigaohm seals, improved seal resistance, and enhanced patch stability. Concentrated stock solutions of all agonists were prepared in pipette solution and stored at  $-80^{\circ}\text{C}$  before each experiment. The external solution contained (in mM) 142 KCl, 5.4 NaCl, 0.2 CaCl<sub>2</sub>, 1.7 MgCl<sub>2</sub>, and 10 HEPES, adjusted to pH 7.4 with NaOH. Patch pipettes were fabricated from type 7052 nonfilamented glass (King Precision Glass) with inner and outer diameters of 1.15 mm and 1.65 mm, respectively, coated with Sylgard 184 (Dow Corning) and heat polished to yield resistances from 5 to 8 M $\Omega$ .

Single-channel currents were recorded using an Axopatch 200B patch-clamp amplifier (Molecular Devices), with the gain set at 100 mV/pA and the internal Bessel filter at 100 kHz, and

sampled at intervals of 2–20  $\mu\text{s}$  using a National Instruments model BNC-2090 A/D converter with a PCI 611e acquisition card and recorded to the hard disk of a PC computer with the program Acquire (Bruxon). Criteria for accepting data for analysis included a patch-clamp noise meter reading of 160–200 fA (root mean squared deviation at 5 kHz bandwidth) and clear temporal separation of clusters of openings arising from a single-receptor channel. Single-channel openings and closings were detected by using the program TAC (Bruxon), with the cutoff frequency of the Gaussian digital filter set to 5 kHz and the detection threshold set to half the unitary current amplitude.

Oxidation and reduction of receptors with substituted cysteine residues were performed as previously described (Mukhtasimova and Sine, 2007; Mukhtasimova et al., 2009). In brief, to carry out oxidative cross-linking, cells were incubated for 5 min in external solution containing 4.4 mM H<sub>2</sub>O<sub>2</sub> and then washed with external solution before establishing a cell-attached gigaohm seal (Mukhtasimova and Sine, 2007). After recording agonist-elicited single-channel currents from receptors subjected to oxidizing conditions, to reverse oxidation, dithiothreitol (DTT) was added to the external solution to achieve a final concentration of 20  $\mu\text{M}$ , while maintaining the cell-attached patch configuration. After addition of DTT, if a change in channel opening was observed, the change occurred within tens of seconds, and a second recording was obtained from the same patch.

Openings and closings above the detection threshold were corrected for the effective filter frequency  $F_c$  (Colquhoun and Sigworth, 1983) and placed into logarithmic bins (Sigworth and Sine, 1987), and the sum of exponentials was fitted to the open and closed-time distributions. The fit of the closed-time distribution was used to establish a critical closed time to distinguish closings within clusters from those between clusters; this critical closed time was determined from the point of intersection between the major agonist-sensitive closed-time component and the succeeding component, as described (Sine et al., 1990). Openings and closings within all clusters were included for analysis, whereas single openings flanked by closings longer than the critical time were excluded. Cluster open probability was defined as the total open time within a cluster divided by the total open plus closed time in the cluster; histograms of cluster open probability were generated using custom software.

### Online supplemental material

Fig. S1 shows that oxidative cross-linking of AChRs with cysteine substituted for  $\alpha\text{D97}$  and  $\alpha\text{Y127}$  does not affect channel opening by partial agonists. Fig. S2 shows that oxidative cross-linking of AChRs with cysteine substituted for  $\alpha\text{D97}$  and  $\alpha\text{K125}$  does not affect channel opening by full or partial agonists or channel opening in the absence of agonist. Fig. S3 shows that oxidative cross-linking of AChRs with cysteine substituted for  $\alpha\text{T51}$  and  $\alpha\text{K125}$  does not affect channel opening by full or partial agonists. Fig. S4 shows that oxidative cross-linking of AChRs with cysteine substituted for  $\alpha\text{L109}$  and  $\alpha\text{YT117}$  suppresses channel opening by suberyldicholine (SubCho) but not that by partial agonists. Fig. S5 shows that oxidative cross-linking of AChRs with cysteine substituted for  $\alpha\text{T32}$  and  $\alpha\text{Q59}$  does not affect channel opening

by partial agonists. Fig. S6 shows that oxidative cross-linking of AChRs with cysteine substituted for  $\alpha$ Q59 and  $\alpha$ T117 does not affect channel opening by full or partial agonists. Table S1 shows mean open durations for different agonists after oxidation and reduction of  $\alpha$ T51C/ $\alpha$ K125C receptors. Table S2 shows mean open durations for different agonists after oxidation and reduction of  $\alpha$ L109C/ $\alpha$ T117C receptors. Table S3 shows mean open durations for different agonists after oxidation and reduction of  $\alpha$ T32C/ $\alpha$ Q59C receptors. Table S4 shows mean open durations for different agonists after oxidation and reduction of  $\alpha$ T32C/ $\alpha$ N159C and  $\alpha$ Q59C/ $\alpha$ T117C receptors.

## Results

### Principal face of the $\alpha$ subunit

Initially we focused on a tetrad of juxtaposed residues at the principal face of the  $\alpha$  subunit:  $\alpha$ Y127 and  $\alpha$ K125 on  $\beta$ -strand 6' that precede  $\alpha$ C128 of the signature cystine loop;  $\alpha$ D97 that follows loop A of the agonist-binding site; and  $\alpha$ T51 from  $\beta$ -strand 2 (Fig. 1). The spatial relationships among these residues are conspicuous, with  $\alpha$ D97 inserting between  $\alpha$ Y127 and  $\alpha$ K125 and  $\alpha$ K125 inserting between  $\alpha$ D97 and  $\alpha$ T51. These spatial relationships are also evident in solved structures of homologous proteins, including the  $\alpha$ 4 $\beta$ 2 AChR (Morales-Perez et al., 2016), the *Torpedo*  $\alpha$ 1 $\beta$  $\gamma$  $\delta$  AChR (Unwin, 2005), the 5-HT<sub>3A</sub> receptor (Hassaine et al., 2014), ACh binding protein (Brejc et al., 2001; Hansen et al., 2005), and the  $\alpha$ 1 ligand-binding domain (Dellisanti et al., 2007). Furthermore, this residue tetrad encompasses three distinct structural regions within the receptor's extracellular domain, the pre-cystine loop, loop A, and  $\beta$ -strand 2; its location between the periphery of the agonist-binding site and the pore domain suggests a role in transducing agonist binding into channel gating.

### The pair $\alpha$ Y127C and $\alpha$ D97C

Studies of the pair  $\alpha$ Y127C and  $\alpha$ D97C illustrate the overall approach and key experimental observations. The mutant  $\alpha$  subunit was coexpressed with complementary  $\beta$ ,  $\epsilon$ , and  $\delta$  subunits in BOSC 23 cells, and single-channel currents were recorded from cell-attached patches with a specified concentration of ACh included within the patch pipette. An intermediate to high concentration of ACh was chosen to elicit readily identifiable clusters of successive channel openings, all from the same receptor, framed by long desensitized closed periods (Sakmann et al., 1980), and was empirically determined for each combination of agonist and mutant receptor. In the presence of 30  $\mu$ M ACh, the  $\alpha$ Y127C/ $\alpha$ D97C mutant receptor exhibited clusters of channel openings composed of two exponential components with mean durations of  $\sim$ 0.2 and 0.8 ms (Table 1) and a cluster mean open probability of  $\sim$ 0.9 (Fig. 2 A). In contrast, after pretreatment with the oxidizing reagent H<sub>2</sub>O<sub>2</sub>, the channel openings comprised a single exponential component with a reduced mean duration of  $\sim$ 0.2 ms (Table 1) and a markedly diminished mean open probability  $<$ 0.1. The effects of oxidation reversed after addition of the reducing reagent DTT to the extracellular solution (Fig. 2 A); however, a few clusters with intermediate open probability remained, likely owing to incomplete reduction of the disulfide

bond between the pair of substituted cysteine residues within each of the two  $\alpha$  subunits per receptor. This procedure of pretreatment with H<sub>2</sub>O<sub>2</sub> followed by application of DTT allowed receptors within the same patch of membrane to be monitored after both oxidation and reduction.

Control recordings from the wild-type AChR in the presence of 30  $\mu$ M ACh revealed mean open durations and cluster mean open probability similar to those from the  $\alpha$ Y127C/ $\alpha$ D97C mutant receptor (Fig. 2 B and Table 1), indicating that the cysteine substitutions minimally affect receptor function. Pretreatment with either H<sub>2</sub>O<sub>2</sub> or H<sub>2</sub>O<sub>2</sub> followed by DTT was without effect, showing that the functional changes after oxidation depend on the presence of the substituted cysteine residues.

As an additional control, we recorded ACh-elicited single-channel currents from receptors with single cysteine substitutions. The single residue mutants,  $\alpha$ D97C and  $\alpha$ Y127C, are loss- and gain-of-function mutations, respectively, unlike the double mutant. As a consequence, the  $\alpha$ D97C mutant was studied using an ACh concentration of 1  $\mu$ M and the  $\alpha$ Y127C mutant with a concentration of 30  $\mu$ M. Pretreatment with either H<sub>2</sub>O<sub>2</sub> or H<sub>2</sub>O<sub>2</sub> followed by DTT did not alter the mean open duration or cluster mean open probability (Fig. 3 and Table 1), showing that the suppression of ACh-elicited single-channel currents after oxidation depends on the presence of both the  $\alpha$ D97C and  $\alpha$ Y127C mutations. Furthermore, if H<sub>2</sub>O<sub>2</sub> chemically modified either of the singly substituted cysteine residues, such modification had no apparent functional consequences.

The changes in receptor function after oxidative cross-linking suggest efficient agonist-elicited channel opening requires displacement of  $\alpha$ Y127 relative to  $\alpha$ D97. To evaluate this possibility, cells expressing the  $\alpha$ Y127C/ $\alpha$ D97C mutant receptor were preincubated with ACh, and then H<sub>2</sub>O<sub>2</sub> was added in the continued presence of ACh before recording ACh-elicited single-channel currents. In contrast to the suppression of channel opening after treatment with H<sub>2</sub>O<sub>2</sub> alone (Fig. 4 A), channel opening remained efficient when H<sub>2</sub>O<sub>2</sub> was applied in the presence of ACh (Fig. 4 B). This observation suggests that in the absence of ACh, the distance between  $\alpha$ Y127C and  $\alpha$ D97C is short enough to allow cross-linking, but in the presence of ACh, the interresidue distance increases beyond that which allows cross-linking.

To determine whether the effect of cross-linking between  $\alpha$ Y127C and  $\alpha$ D97C depends on agonist efficacy, we recorded single-channel currents elicited by a series of agonists ranging in efficacy. For another strong agonist, suberyldicholine (Sub-Cho), pretreatment with H<sub>2</sub>O<sub>2</sub> suppressed channel opening, as observed for ACh, and efficient channel opening was restored after addition of DTT (Fig. 5 A and Table 1). However, for the partial agonist dimethyl-piperazinium (PIP), channel opening was unaffected by pretreatment with H<sub>2</sub>O<sub>2</sub> (Fig. 5 B and Table 1). Furthermore, for carbamylcholine (CCh), a partial agonist structurally similar to ACh, and tetramethylammonium (TMA) and choline (Cho), two weak agonists that mirror substructures within ACh, channel opening was unaffected by pretreatment with H<sub>2</sub>O<sub>2</sub> (Fig. S1, A-C; and Table 1). Control recordings from wild-type receptors activated by each agonist showed no changes after treatment with either H<sub>2</sub>O<sub>2</sub> or H<sub>2</sub>O<sub>2</sub> followed by DTT (Fig. S1, D-G; and Table 1). Notably, the relative efficacy of

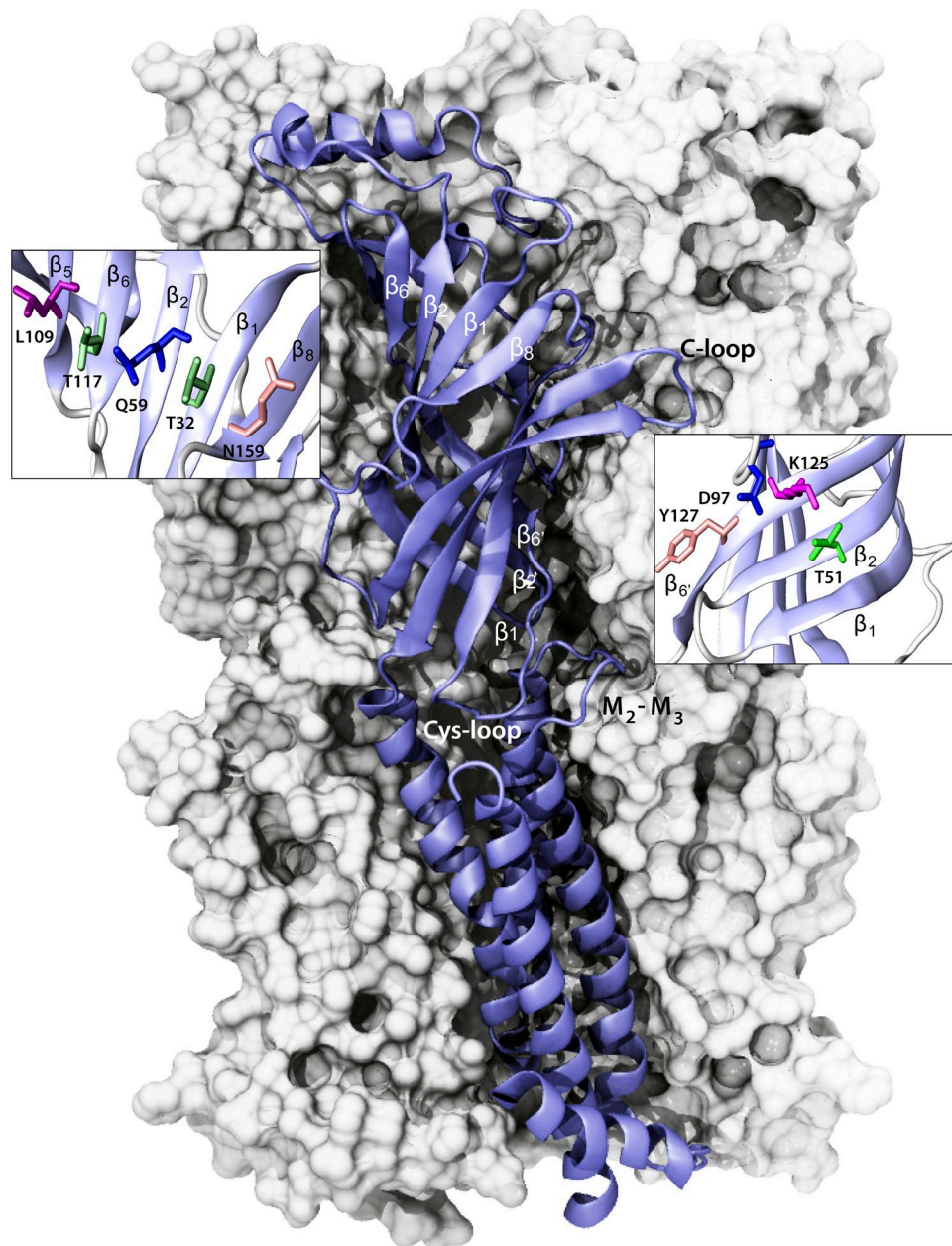


Figure 1. **Structural bases for generating pairwise cysteine substitutions.** X-ray structure of the heteromeric  $\alpha_4\beta_2$  nicotinic AChR (Morales-Perez et al., 2016; PDB accession no. 5KXI) with one of the  $\alpha_4$  subunits shown in secondary structure representation (purple). Insets show residues subjected to cysteine substitution from the principal (right) and complementary (left) faces of the  $\alpha_1$  subunit (Dellisanti et al., 2007; PDB accession no. 2QCI).

the six agonists was maintained in the double-mutant receptors, further showing that the mutations minimally affect receptor function. The overall results show that, in contrast to full agonists, channel opening by partial agonists was not affected by cross-linking between  $\alpha Y127C$  and  $\alpha D97C$ .

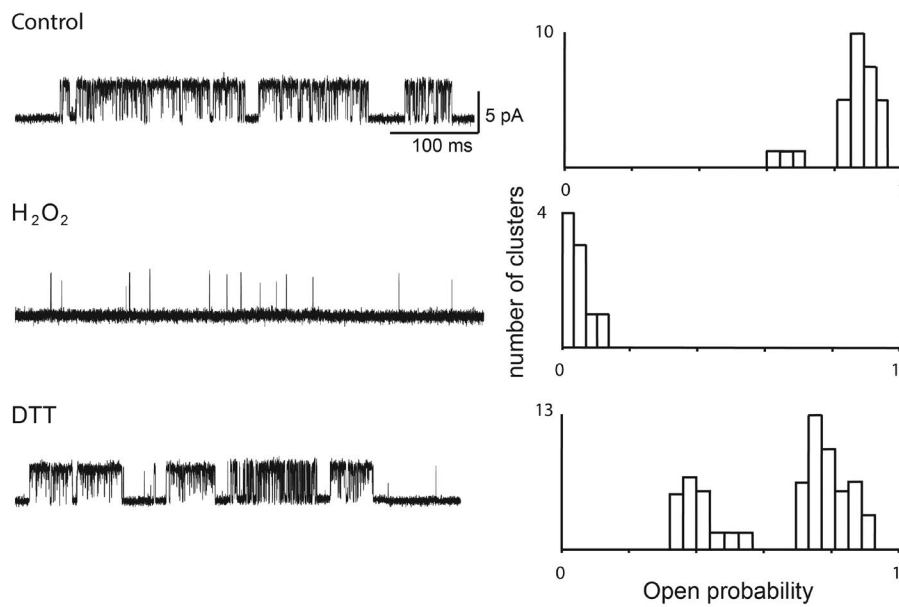
As an additional control, we recorded Cho-elicited single-channel currents from receptors with single-cysteine substitutions. Pretreatment with either  $H_2O_2$  or  $H_2O_2$  followed by DTT did not alter the mean open duration or cluster mean open probability for receptors with either the  $\alpha D97C$  or  $\alpha Y127C$  mutations (Fig. S1, H and I; and Table 1). Furthermore, if  $H_2O_2$  chemically modified either of the singly substituted cysteine

residues, the modifications did not affect Cho-elicited single-channel currents.

#### The pair $\alpha K125C$ and $\alpha D97C$

In the presence of the nominally weak agonist Cho, the  $\alpha K125C/\alpha D97C$  mutant receptor exhibited both long-lived and brief channel openings (Table 2), and the cluster mean open probability spanned from low to high probability (Fig. 6 A). Control recordings from the wild-type AChR activated by Cho revealed uniformly brief channel openings and low cluster mean open probability distributed over a narrow range (Fig. 6 B and Table 2), indicating the  $\alpha K125C/\alpha D97C$  mutant promotes a gain of function

### A $\alpha$ D97C/ $\alpha$ Y127C 30 $\mu$ M ACh



### B Wild-type 30 $\mu$ M ACh

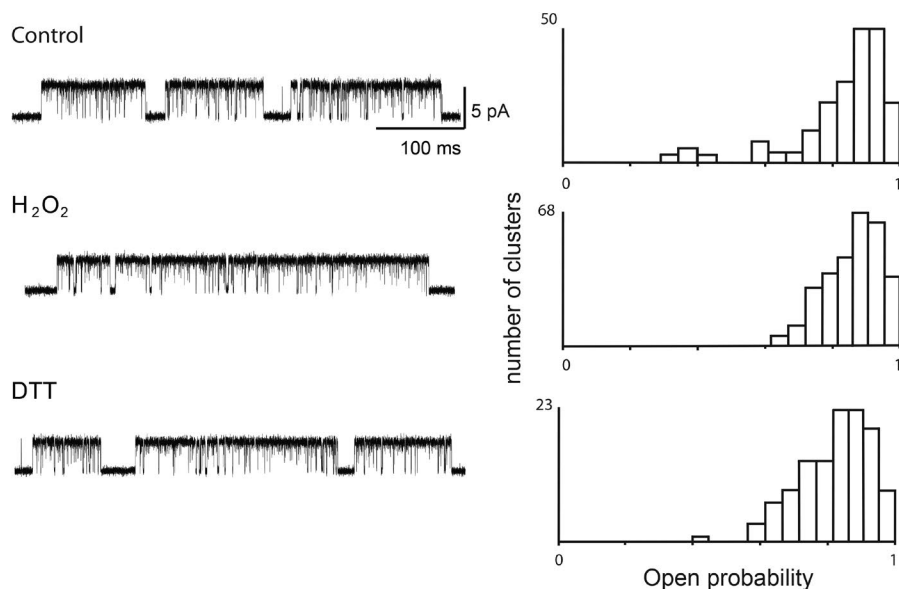


**Figure 2. Oxidative cross-linking of AChRs with cysteine substituted for  $\alpha$ D97 and  $\alpha$ Y127 suppresses channel opening by ACh.** (A) Single-channel currents from the  $\alpha$ D97C/ $\alpha$ Y127C mutant receptor were recorded in the presence of the indicated concentration of ACh under control conditions (top trace), after pretreatment with  $H_2O_2$  (middle trace), or after successive treatment with  $H_2O_2$  and DTT (bottom trace); the middle and bottom traces were obtained from the same membrane patch. See Materials and methods for the procedure to pretreat and remove  $H_2O_2$  and apply DTT. Individual clusters of channel openings, all from the same AChR channel, are shown at a bandwidth of 5 kHz (Gaussian response). To the right of each trace is a histogram of open probability of individual clusters collected over the entire recording; clusters were defined by using an intercluster closed interval determined from a histogram of all closed intervals (Materials and methods). (B) Recordings and histograms of cluster open probability for the wild-type adult human receptor, as in A.

with Cho as the agonist. Moreover, pretreating the  $\alpha$ K125C/ $\alpha$ D97C mutant receptor with  $H_2O_2$  eliminated long-lived channel openings, and the remaining channel openings were brief and the mean open probability markedly diminished. Subsequent application of DTT restored long-lived channel openings and increased the open probability. Recordings from the wild-type AChR activated by Cho showed that neither  $H_2O_2$  nor subsequent treatment with DTT affects channel opening (Fig. 6 B). Thus with Cho as the agonist, receptors containing the  $\alpha$ K125C/ $\alpha$ D97C mutant showed a gain of function relative to the wild-type receptor, and this gain was countered by oxidative cross-linking.

In the presence of the full agonist ACh, the  $\alpha$ K125C/ $\alpha$ D97C mutant receptor exhibited both long-lived and brief channel openings (Table 2), and the cluster mean open probability

spanned a wide range (Fig. S2 A); both functional measures mirrored those by Cho, so for this mutant receptor ACh and Cho are similarly efficacious, and the distinction between full and partial agonist is lost. However, neither pretreatment with  $H_2O_2$  nor subsequent treatment with DTT affected ACh-elicited channel openings. Similarly, for the strong agonist SubCho and the weak agonists CCh, PIP, and TMA, pretreatment with  $H_2O_2$  did not affect channel opening (Fig. S2, B-E; and Table 2). Thus, in contrast to the suppression of Cho-elicited channel opening by cross-linking between  $\alpha$ K125C and  $\alpha$ D97C, channel opening elicited by a range of full and partial agonists was unaffected by cross-linking; the structure of Cho, rather than its efficacy, is likely decisive in the suppression of channel opening by cross-linking.

Table 1. Mean open durations for different agonists after oxidation and reduction of  $\alpha$ D97C/ $\alpha$ Y127C receptors

Agonist/receptor (number of transfections)	Treatment (number of patches)	mOpen <sub>1</sub>	Area <sub>1</sub>	mOpen <sub>2</sub>	Area <sub>2</sub>
ACh/ $\alpha$ D97C/ $\alpha$ Y127C (8)	Control (4)	$2.3 \pm 0.3 \times 10^{-4}$	$0.4 \pm 0.08$	$8.0 \pm 0.8 \times 10^{-4}$	$0.7 \pm 0.10$
	H <sub>2</sub> O <sub>2</sub> (12)	$2.0 \pm 0.1 \times 10^{-4}$	$1.0 \pm 0.03$		
	DTT (8)	$3.0 \pm 0.1 \times 10^{-4}$	$0.6 \pm 0.04$	$8.5 \pm 0.1 \times 10^{-4}$	$0.4 \pm 0.06$
ACh/wild type (3)	Control (4)	$1.9 \pm 0.1 \times 10^{-5}$	$0.2 \pm 0.05$	$1.2 \pm 0.1 \times 10^{-3}$	$0.8 \pm 0.08$
	H <sub>2</sub> O <sub>2</sub> (8)	$2.0 \pm 0.2 \times 10^{-5}$	$0.1 \pm 0.01$	$1.3 \pm 0.1 \times 10^{-3}$	$0.9 \pm 0.09$
	DTT (6)	$1.8 \pm 0.1 \times 10^{-5}$	$0.2 \pm 0.04$	$9.4 \pm 0.7 \times 10^{-4}$	$0.7 \pm 0.06$
SubCho/ $\alpha$ D97C/ $\alpha$ Y127C (5)	Control (6)			$6.5 \pm 0.5 \times 10^{-4}$	$1.0 \pm 0.02$
	H <sub>2</sub> O <sub>2</sub> (12)	$6.9 \pm 0.1 \times 10^{-5}$	$0.2 \pm 0.04$	$1.8 \pm 0.5 \times 10^{-4}$	$0.8 \pm 0.06$
	DTT (8)			$5.4 \pm 0.6 \times 10^{-4}$	$1.0 \pm 0.02$
SubCho/wild type (3)	Control (4)	$2.6 \pm 0.14 \times 10^{-5}$	$0.3 \pm 0.05$	$2.9 \pm 0.2 \times 10^{-4}$	$0.7 \pm 0.08$
	H <sub>2</sub> O <sub>2</sub> (4)	$1.9 \pm 0.11 \times 10^{-5}$	$0.4 \pm 0.06$	$2.8 \pm 0.1 \times 10^{-4}$	$0.6 \pm 0.09$
	DTT (4)	$2.1 \pm 0.14 \times 10^{-5}$	$0.3 \pm 0.05$	$2.7 \pm 0.1 \times 10^{-4}$	$0.7 \pm 0.10$
CCh/ $\alpha$ D97C/ $\alpha$ Y127C (3)	Control (4)	$7.3 \pm 0.2 \times 10^{-5}$	$0.8 \pm 0.07$	$1.8 \pm 0.8 \times 10^{-4}$	$0.3 \pm 0.07$
	H <sub>2</sub> O <sub>2</sub> (6)	$6.0 \pm 0.9 \times 10^{-5}$	$0.7 \pm 0.06$	$2.8 \pm 0.1 \times 10^{-4}$	$0.3 \pm 0.04$
	DTT (8)	$4.9 \pm 0.5 \times 10^{-5}$	$0.7 \pm 0.06$	$2.3 \pm 0.2 \times 10^{-4}$	$0.3 \pm 0.05$
CCh/wild type (3)	Control (4)			$3.2 \pm 0.3 \times 10^{-4}$	$1.0 \pm 0.03$
	H <sub>2</sub> O <sub>2</sub> (6)			$3.1 \pm 0.3 \times 10^{-4}$	$1.0 \pm 0.02$
	DTT (4)			$2.9 \pm 0.3 \times 10^{-4}$	$1.0 \pm 0.03$
PIP/ $\alpha$ D97C/ $\alpha$ Y127C (3)	Control (4)			$2.1 \pm 0.1 \times 10^{-4}$	$1.0 \pm 0.03$
	H <sub>2</sub> O <sub>2</sub> (6)			$2.1 \pm 0.5 \times 10^{-4}$	$1.0 \pm 0.02$
	DTT (6)			$2.2 \pm 0.7 \times 10^{-4}$	$1.0 \pm 0.05$
PIP/wild type (3)	Control (4)			$2.5 \pm 0.2 \times 10^{-4}$	$1.0 \pm 0.04$
	H <sub>2</sub> O <sub>2</sub> (4)			$2.9 \pm 0.2 \times 10^{-4}$	$1.0 \pm 0.03$
	DTT (4)			$2.9 \pm 0.2 \times 10^{-4}$	$1.0 \pm 0.03$
TMA/ $\alpha$ D97C/ $\alpha$ Y127C (3)	Control (4)			$3.8 \pm 1.0 \times 10^{-4}$	$1.0 \pm 0.02$
	H <sub>2</sub> O <sub>2</sub> (6)			$4.1 \pm 0.3 \times 10^{-4}$	$1.0 \pm 0.03$
	DTT (4)			$3.8 \pm 0.5 \times 10^{-4}$	$1.0 \pm 0.03$
TMA/wild type (3)	Control (4)			$3.9 \pm 0.4 \times 10^{-4}$	$1.0 \pm 0.03$
	H <sub>2</sub> O <sub>2</sub> (4)			$4.1 \pm 0.2 \times 10^{-4}$	$1.0 \pm 0.03$
	DTT (4)			$3.9 \pm 0.3 \times 10^{-4}$	$1.0 \pm 0.05$
Cho/ $\alpha$ D97C/ $\alpha$ Y127C (4)	Control (4)			$2.1 \pm 0.2 \times 10^{-4}$	$1.0 \pm 0.03$
	H <sub>2</sub> O <sub>2</sub> (8)			$2.0 \pm 0.3 \times 10^{-4}$	$1.0 \pm 0.03$
	DTT (6)			$2.2 \pm 0.7 \times 10^{-4}$	$1.0 \pm 0.04$

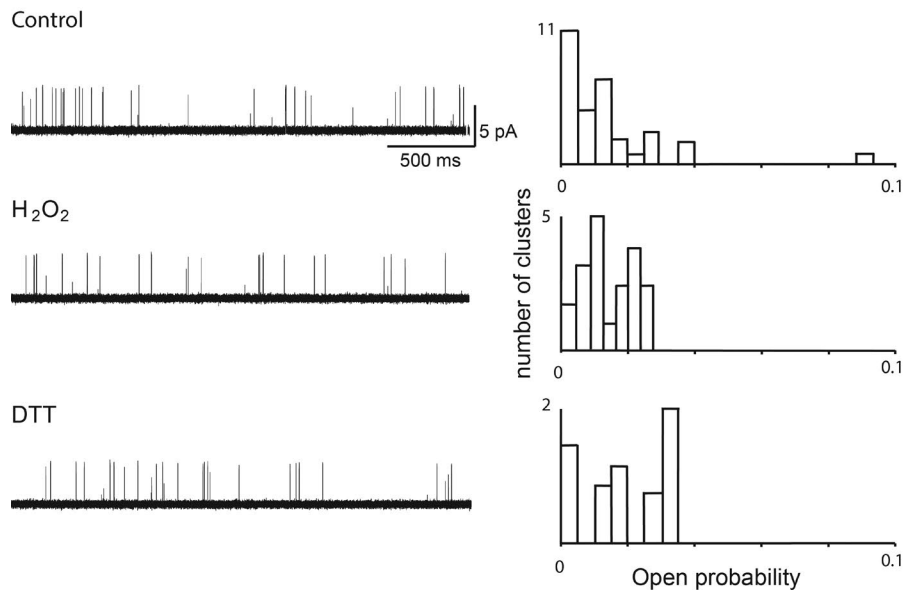
For each agonist/receptor/treatment combination, mean open durations and relative areas from a fit of the sum of exponentials were determined. Values listed are the mean  $\pm$  SD for the indicated number of patches.

As a control, we recorded Cho-elicited single-channel currents from receptors with the single-cysteine substitution  $\alpha$ K125C. As observed for receptors with the single-cysteine substitution  $\alpha$ D97C (Fig. S1 H), pretreatment of the  $\alpha$ K125C receptor with either H<sub>2</sub>O<sub>2</sub> or DTT did not alter the mean open duration or cluster mean open probability (Fig. S2 F and Table 2). Furthermore, if H<sub>2</sub>O<sub>2</sub> chemically modified the single substituted cysteine residue, any effects of the modification were not apparent in Cho-elicited single-channel currents. Thus, the suppression of

Cho-elicited single-channel currents by oxidation depends on the presence of both the  $\alpha$ D97C and  $\alpha$ K125C mutations.

The  $\alpha$ K125C/ $\alpha$ D97C mutant receptor also exhibited brief channel openings in the absence of agonist, unlike the wild-type or other mutant receptors examined herein. Neither pretreatment with H<sub>2</sub>O<sub>2</sub> nor subsequent addition of DTT affected channel opening of the  $\alpha$ K125C/ $\alpha$ D97C mutant receptor in the absence of agonist (Fig. S2 G). Thus, cross-linking between  $\alpha$ K125C and  $\alpha$ D97C did not affect structural changes that underlie spontaneous channel opening.

### A $\alpha$ D97C 1 $\mu$ M ACh



### B $\alpha$ Y127C 30 $\mu$ M ACh

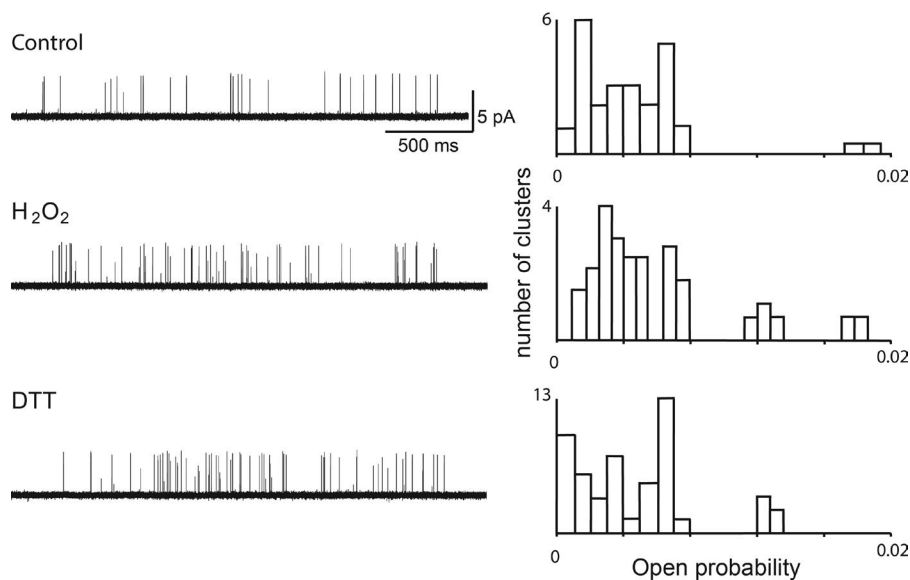


**Figure 3. Receptors in which cysteine was substituted for a single residue are unaffected by H<sub>2</sub>O<sub>2</sub> or DTT. (A)** Single-channel currents from the  $\alpha$ D97C mutant receptor were recorded in the presence of the indicated concentration of ACh under control conditions (top trace), after pretreatment with H<sub>2</sub>O<sub>2</sub> (middle trace), or after successive treatment with H<sub>2</sub>O<sub>2</sub> and DTT (bottom trace). **(B)** Single-channel currents from the  $\alpha$ Y127C mutant receptor were recorded in the presence of the indicated concentration of ACh under control conditions (top trace), after pretreatment with H<sub>2</sub>O<sub>2</sub> (middle trace), or after successive treatment with H<sub>2</sub>O<sub>2</sub> and DTT (bottom trace). To the right of each trace is a histogram of open probability of individual clusters collected over the entire recording, as in Fig. 2.

Finally, channel opening by the  $\alpha$ K125C/ $\alpha$ D97C receptor was suppressed regardless of whether H<sub>2</sub>O<sub>2</sub> was applied in the absence or presence of Cho (unpublished data), in contrast to the  $\alpha$ Y127C/ $\alpha$ D97C mutant receptor treated with H<sub>2</sub>O<sub>2</sub> in the presence of ACh. Thus, the distance between  $\alpha$ K125C and  $\alpha$ D97C remained short enough for cross-linking in the presence or absence of Cho.

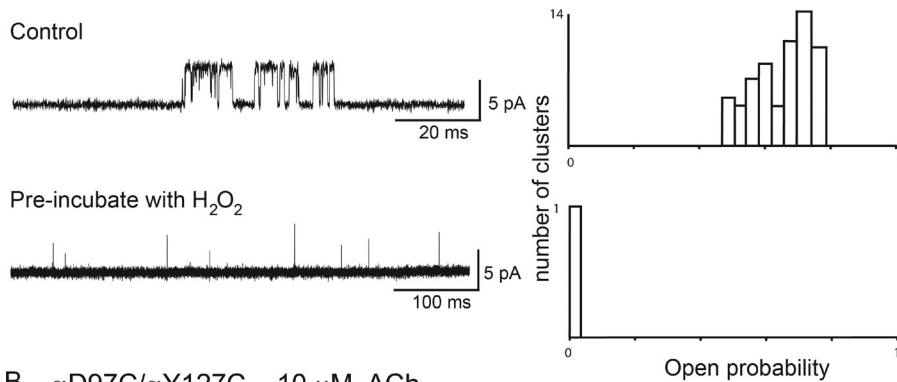
#### The pair $\alpha$ K125C and $\alpha$ T51C

In the presence of 0.3  $\mu$ M ACh, the  $\alpha$ K125C/ $\alpha$ T51C mutant receptor exhibited brief channel openings (Table S1), and the cluster mean open probability distributed over a narrow range <0.1 (Fig. 7A). However, pretreatment with H<sub>2</sub>O<sub>2</sub> markedly prolonged channel openings (Table S1), and the cluster mean open probability increased and distributed over a wide range. Subsequent

treatment with DTT restored brief channel openings and low cluster mean open probability. Thus, cross-linking between  $\alpha$ K125C and  $\alpha$ T51C enhanced channel opening in a reversible manner. Of the pairwise cysteine mutants tested herein, the  $\alpha$ K125C/ $\alpha$ T51C mutant was unique in that cross-linking enhanced rather than suppressed agonist-elicited channel opening.

In the presence of the strong agonist SubCho, the  $\alpha$ K125C/ $\alpha$ T51C mutant receptor exhibited long-lived channel openings and high cluster mean open probability spanning a wide range (Fig. S3 A and Table S1), in contrast to the brief channel openings and low open probability observed in the presence of ACh. However, neither pretreatment with H<sub>2</sub>O<sub>2</sub> nor subsequent treatment with DTT affected the channel open time or open probability. Thus, unlike channel opening elicited by ACh, cross-linking between  $\alpha$ K125C and  $\alpha$ T51C did not enhance channel opening by SubCho.

**A**  $\alpha$ D97C/ $\alpha$ Y127C 10  $\mu$ M ACh



**B**  $\alpha$ D97C/ $\alpha$ Y127C 10  $\mu$ M ACh

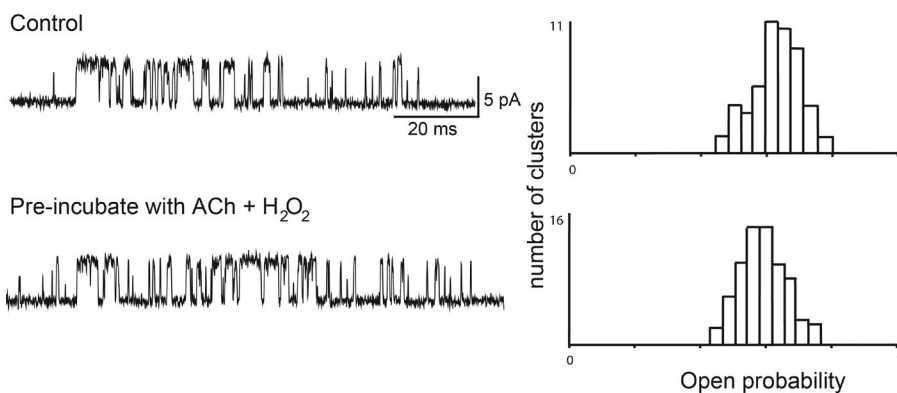


**Figure 4. Preincubation with ACh prevents oxidative cross-linking of the  $\alpha$ D97C/ $\alpha$ Y127C mutant.** (A) Single-channel currents from the  $\alpha$ D97C/ $\alpha$ Y127C mutant receptor were recorded under control conditions (top trace), or after preincubation with  $H_2O_2$  (bottom trace). (B) Single-channel currents were recorded in the presence of ACh under control conditions (top trace), or after successive preincubation with ACh and then  $H_2O_2$  in the continued presence of ACh (bottom trace). The concentration of ACh was 10  $\mu$ M during the preincubation and subsequent single-channel recording. To the right of each trace is a histogram of cluster open probability, as in Fig. 2.

In the presence of the partial agonists CCh, PIP, TMA, or Cho, the  $\alpha$ K125C/ $\alpha$ T51C mutant receptor exhibited brief channel openings and low cluster mean open probability, analogous to ACh. Of the partial agonists tested against the  $\alpha$ K125C/ $\alpha$ T51C mutant receptor, only CCh showed an obvious loss of function because of the mutations (compare Figs. S1 F with S3 B), whereas channel opening by PIP, TMA, and Cho was similar to that observed for the wild-type receptor (compare Figs. S1 E with 7 B, Figs. S1 G with S3 C, and Figs. 6 B with S3 D). Moreover, neither pretreatment by  $H_2O_2$  nor subsequent treatment with DTT affected channel opening elicited by any of these partial agonists (Fig. 7 B; Fig. S3, B–D; and Table S1). Thus, cross-linking between  $\alpha$ K125C and  $\alpha$ T51C enhanced channel opening elicited by ACh but not that by SubCho nor any of the partial agonists. Thus, the structure of ACh, rather than its efficacy, was decisive in the enhancement of channel opening mediated by cross-linking.

As a control, we recorded single-channel currents elicited by either ACh or Cho from receptors with the single-cysteine substitution  $\alpha$ T51C. As observed for the single-cysteine substitution  $\alpha$ K125C (Fig. S2 F), neither pretreatment  $H_2O_2$  nor DTT altered the mean open duration or cluster mean open probability of receptors with the single-cysteine substitution  $\alpha$ T51C (Fig. S3, E and F; and Table S1). Furthermore, if  $H_2O_2$  chemically modified the single substituted cysteine residue, any effects of the modification were not apparent in either ACh- or Cho-elicited single-channel currents. Thus, the enhancement of ACh-elicited single-channel currents after

oxidation depended on the presence of both the  $\alpha$ T51C and  $\alpha$ K125C mutations.

**Complementary face of the  $\alpha$  subunit**

At the complementary face of the  $\alpha$  subunit, five residues align in a contiguous stripe:  $\alpha$ L109 and  $\alpha$ T117 on antiparallel  $\beta$ -strands 5' and 6, respectively, which give rise to a  $\beta$  hairpin at the top of the subunit;  $\alpha$ Q59 and  $\alpha$ T32 on antiparallel  $\beta$ -strands 2 and 1, respectively, which give rise to a  $\beta$  hairpin at the interface between the extracellular and pore domains; and  $\alpha$ N159 on  $\beta$ -strand 9, which run parallel to  $\beta$ -strand 1 (Fig. 1). The spatial relationships among these residues mirror those from solved structures of homologous proteins, including the  $\alpha 4\beta 2$  receptor (Morales-Perez et al., 2016), the *Torpedo*  $\alpha 1\beta\gamma\delta$  receptor (Unwin, 2005), the 5-HT<sub>3A</sub> receptor (Hassaine et al., 2014), ACh binding protein (Brejc et al., 2001; Hansen et al., 2005), and the  $\alpha 1$  ligand-binding domain (Dellisanti et al., 2007).

**The pair  $\alpha$ L109C and  $\alpha$ T117C**

In the presence of 30  $\mu$ M ACh, the  $\alpha$ L109C/ $\alpha$ T117C mutant receptor exhibited clusters of channel openings composed of a single exponential component with a mean duration of  $\sim 0.9$  ms (Table S2) and a cluster mean open probability that spanned a wide range (Fig. 8 A). However, pretreatment with  $H_2O_2$  markedly shortened the mean open duration to  $\sim 0.15$  ms (Table S2), reduced the open probability to  $< 0.1$  (Fig. 8 A), and reduced the incidence of clusters. Subsequent addition of DTT restored the

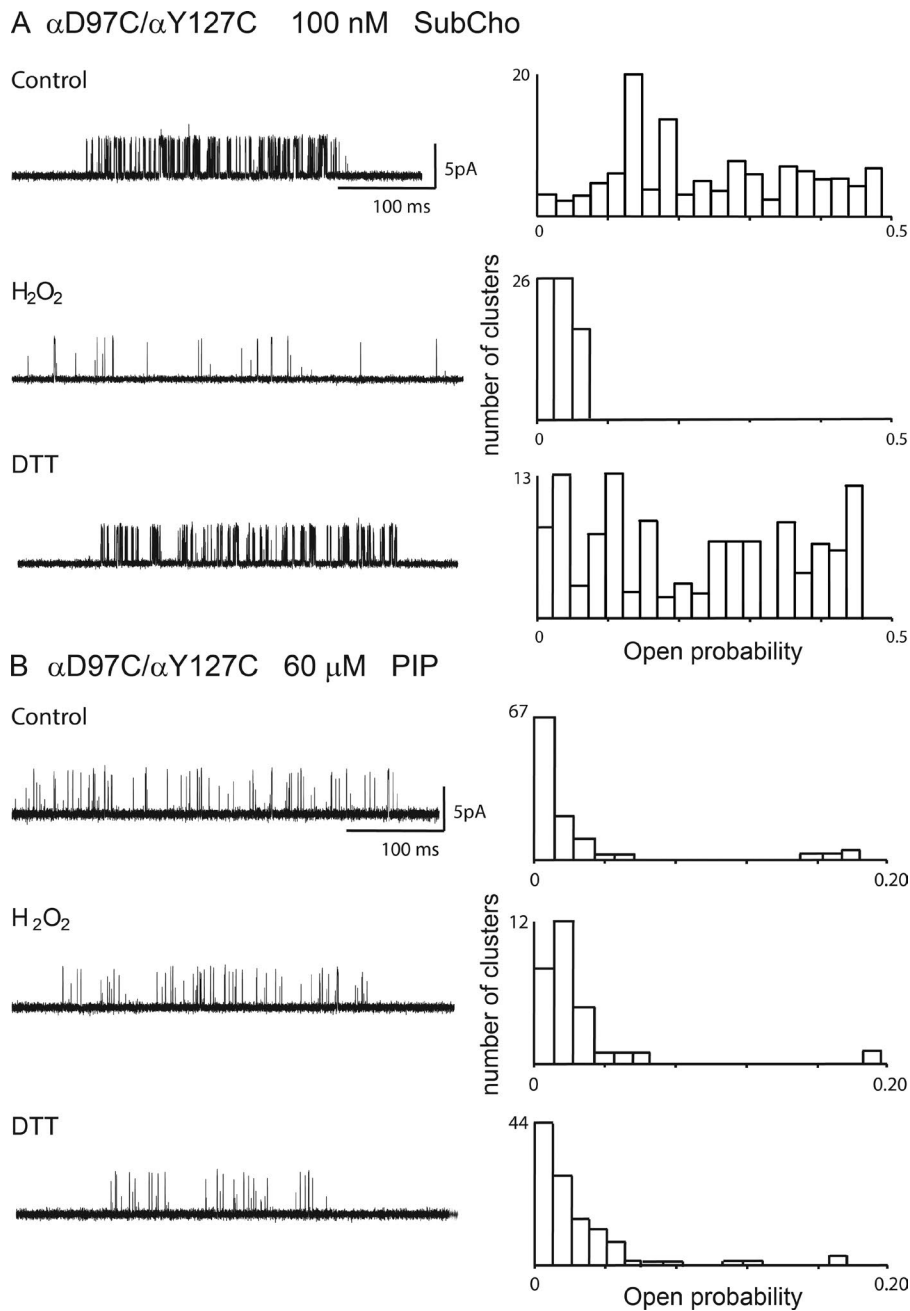


**Figure 5. Oxidative cross-linking of AChRs with cysteine substituted for  $\alpha$ D97 and  $\alpha$ Y127 suppresses channel opening by SubCho but not PIP. (A)** Single-channel currents from the  $\alpha$ D97C/ $\alpha$ Y127C mutant receptor in the presence of SubCho were recorded under control conditions (top trace), after pretreatment with  $H_2O_2$  (middle trace), or after successive treatment with  $H_2O_2$  and DTT (bottom trace); the middle and bottom traces were obtained from the same membrane patch. Histograms of cluster open probability were generated as in Fig. 2. **(B)** Same as in A, but with PIP as the agonist.

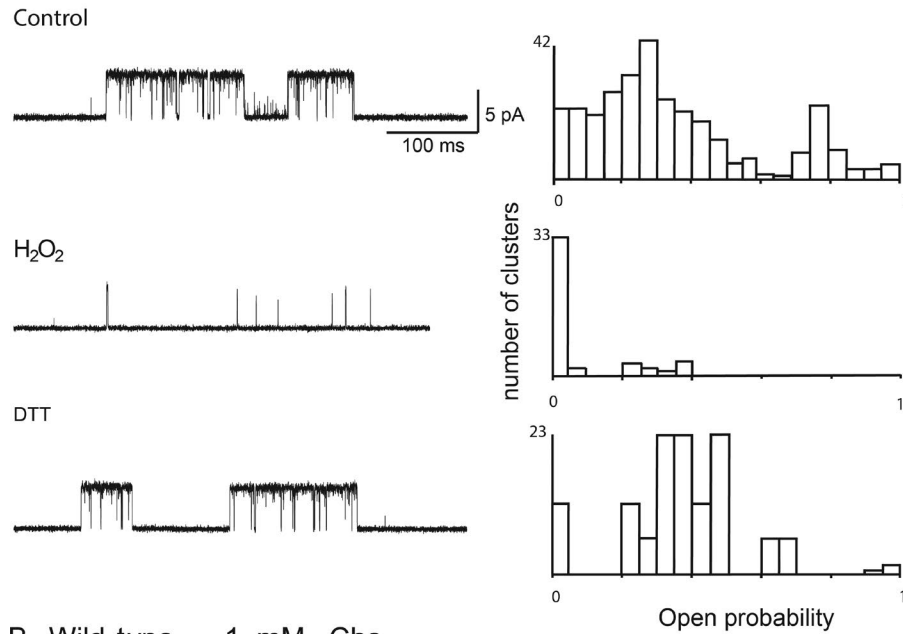
longer mean open duration and the wide range of cluster open probability and increased the incidence of clusters. Analogous recordings in the presence of the strong agonist SubCho revealed qualitatively similar results (Fig. S4 A and Table S2). Thus, cross-linking between  $\alpha$ L109C and  $\alpha$ T117C markedly suppressed channel opening by the strong agonists ACh and SubCho.

In the presence of the partial agonists PIP or CCh, the  $\alpha$ L109C/ $\alpha$ T117C mutant receptor exhibited brief and long channel openings that distributed over a wide range of cluster mean open probability (Table S2 and Figs. 8 B and S4 B). However, pretreatment with  $H_2O_2$  was without effect, in contrast to the strong agonists. The weakest agonists, Cho and TMA, elicited channel openings with a low cluster mean open probability  $<0.1$ , in contrast to ACh, SubCho, CCh, and PIP.

Nevertheless, pretreatment with  $H_2O_2$  did not affect channel opening by TMA or Cho (Fig. S4, C and D; and Table S2). Thus, cross-linking between  $\alpha$ L109C and  $\alpha$ T117C, which stems from antiparallel  $\beta$  strands that form a shared  $\beta$  hairpin at the top of the subunit, suppressed channel opening by full but not partial agonists.

As a control, we recorded single-channel currents elicited by either ACh or Cho from receptors with the single-cysteine substitution  $\alpha$ T117C. Pretreatment of  $\alpha$ T117C receptors with either  $H_2O_2$  or DTT did not alter the mean open duration or cluster mean open probability for either ACh or Cho (Fig. S4, E and F; and Table S2). Thus, if  $H_2O_2$  chemically modified the  $\alpha$ T117C substitution, any effects of the modification were not apparent in either ACh- or Cho-elicited single-channel currents.

**A**  $\alpha$ D97C/ $\alpha$ Y127C 300  $\mu$ M Cho



**B** Wild-type 1 mM Cho

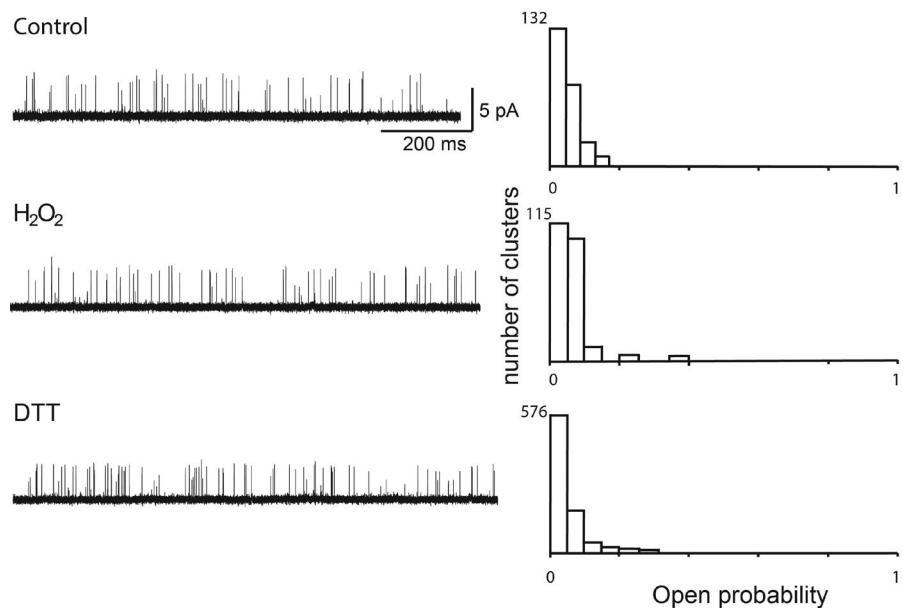


**Figure 6. Oxidative cross-linking of AChRs with cysteine substituted for  $\alpha$ D97 and  $\alpha$ K125 suppresses channel opening by Cho.** (A) Single-channel currents from the  $\alpha$ D97C/ $\alpha$ K125C mutant receptor were recorded in the presence of Cho under control conditions (top trace), after pretreatment with  $H_2O_2$  (middle trace), or after successive treatment with  $H_2O_2$  and DTT (bottom trace); the middle and bottom traces were obtained from the same membrane patch. Individual clusters of channel openings, all from the same AChR channel, are shown at a bandwidth of 5 kHz (Gaussian response). To the right of each trace is a histogram of cluster open probability as in Fig. 2. (B) Recordings and analyses for the wild-type adult human AChR activated by Cho, as in A.

**The pair  $\alpha$ T32C and  $\alpha$ Q59C**

In the presence of 30  $\mu$ M ACh, the  $\alpha$ T32C/ $\alpha$ Q59C mutant receptor exhibited brief and long channel openings and a cluster mean open probability  $<0.1$  (Table S3 and Fig. 9 A). Thus, compared with the wild-type receptor activated by ACh, the  $\alpha$ T32C/ $\alpha$ Q59C mutant conferred a loss of function. Moreover, pretreatment with  $H_2O_2$  reduced the incidence of channel openings, whereas the openings that remained comprised a single brief exponential component with a mean duration of 0.1 ms and a low cluster mean open probability  $<0.1$ . In addition, after establishing a gigaohm seal on a cell pretreated with  $H_2O_2$ , addition of DTT to the extracellular solution markedly increased the incidence of channel openings, and the mean open durations and open

probability approached those of the untreated controls (Fig. 9 A and Table S3).

For SubCho, CCh, TMA, and Cho, the  $\alpha$ T32C/ $\alpha$ Q59C mutant receptor exhibited brief and long channel openings (Table S3) and a low cluster mean open probability, as observed for ACh. Thus, for these agonists the mutations conferred loss of function compared with the wild-type receptor (compare Tables 1 with S3), as observed for ACh. However, neither pretreatment with  $H_2O_2$  nor subsequent treatment with DTT affected channel opening by any of these agonists (Fig. 9 B; Fig. S5, B–D; and Table S3). PIP, on the other hand, elicited robust channel opening of the  $\alpha$ T32C/ $\alpha$ Q59C mutant receptor, but again, neither  $H_2O_2$  nor subsequent treatment with DTT affected channel

Table 2. Mean open durations for different agonists after oxidation and reduction of  $\alpha$ D97C/ $\alpha$ K125C receptors

Agonist/receptor (number of transfections)	Treatment (number of patches)	mOpen <sub>1</sub>	Area <sub>1</sub>	mOpen <sub>2</sub>	Area <sub>2</sub>	mOpen <sub>3</sub>	Area <sub>3</sub>
Cho/wild type (3)	Control (4)			$2.3 \pm 0.3 \times 10^{-4}$	$1.0 \pm 0.03$		
	H <sub>2</sub> O <sub>2</sub> (6)			$2.2 \pm 0.2 \times 10^{-4}$	$1.0 \pm 0.03$		
	DTT (4)			$1.9 \pm 0.2 \times 10^{-4}$	$1.0 \pm 0.05$		
Cho/ $\alpha$ D97C/ $\alpha$ K125C (6)	Control (4)	$3.3 \pm 1.0 \times 10^{-5}$	$0.3 \pm 0.04$	$6.8 \pm 0.4 \times 10^{-4}$	$0.6 \pm 0.07$	$3.3 \pm 0.2 \times 10^{-3}$	$0.05 \pm 0.01$
	H <sub>2</sub> O <sub>2</sub> (6)	$4.1 \pm 0.4 \times 10^{-5}$	$0.8 \pm 0.03$	$1.9 \pm 0.8 \times 10^{-4}$	$0.2 \pm 0.09$		
	DTT (6)	$3.7 \pm 0.7 \times 10^{-5}$	$0.3 \pm 0.06$	$7.3 \pm 0.3 \times 10^{-4}$	$0.6 \pm 0.03$	$4.4 \pm 0.1 \times 10^{-3}$	$0.1 \pm 0.02$
Cho/ $\alpha$ Y125C (1)	Control (4)	$2.4 \pm 0.3 \times 10^{-5}$	$0.4 \pm 0.08$	$2.7 \pm 0.2 \times 10^{-4}$	$0.6 \pm 0.08$		
	H <sub>2</sub> O <sub>2</sub> (6)	$3.1 \pm 0.5 \times 10^{-5}$	$0.4 \pm 0.04$	$2.7 \pm 0.3 \times 10^{-4}$	$0.6 \pm 0.04$		
	DTT (4)	$3.1 \pm 0.6 \times 10^{-5}$	$0.3 \pm 0.06$	$2.6 \pm 0.4 \times 10^{-4}$	$0.6 \pm 0.06$		
ACh/ $\alpha$ D97C/ $\alpha$ K125C (3)	Control (6)	$3.9 \pm 0.2 \times 10^{-5}$	$0.3 \pm 0.02$	$1.2 \pm 0.8 \times 10^{-4}$	$0.3 \pm 0.02$	$3.1 \pm 0.10 \times 10^{-3}$	$0.4 \pm 0.05$
	H <sub>2</sub> O <sub>2</sub> (8)	$2.7 \pm 0.9 \times 10^{-5}$	$0.2 \pm 0.05$	$1.9 \pm 1.0 \times 10^{-4}$	$0.3 \pm 0.04$	$3.2 \pm 0.7 \times 10^{-3}$	$0.5 \pm 0.04$
	DTT (6)	$1.7 \pm 0.5 \times 10^{-5}$	$0.1 \pm 0.03$	$2.2 \pm 0.2 \times 10^{-4}$	$0.2 \pm 0.02$	$6.0 \pm 0.1 \times 10^{-3}$	$0.6 \pm 0.05$
ACh/ $\alpha$ Y125C (3)	Control (4)	$5.8 \pm 0.7 \times 10^{-5}$	$0.3 \pm 0.06$	$4.5 \pm 0.3 \times 10^{-4}$	$0.7 \pm 0.06$		
	H <sub>2</sub> O <sub>2</sub> (4)	$6.0 \pm 0.1 \times 10^{-5}$	$0.3 \pm 0.05$	$4.8 \pm 0.2 \times 10^{-4}$	$0.7 \pm 0.05$		
	DTT (4)	$5.4 \pm 0.1 \times 10^{-5}$	$0.3 \pm 0.04$	$4.6 \pm 0.5 \times 10^{-4}$	$0.7 \pm 0.06$		
SubCho/ $\alpha$ D97C/ $\alpha$ K125C (6)	Control (4)	$8.0 \pm 0.7 \times 10^{-5}$	$0.6 \pm 0.02$	$5.1 \pm 0.4 \times 10^{-4}$	$0.4 \pm 0.02$	$1.4 \pm 0.3 \times 10^{-2}$	$0.02 \pm 0.01$
	H <sub>2</sub> O <sub>2</sub> (6)	$8.3 \pm 0.2 \times 10^{-5}$	$0.6 \pm 0.03$	$7.4 \pm 0.9 \times 10^{-4}$	$0.4 \pm 0.01$	$1.2 \pm 0.5 \times 10^{-2}$	$0.02 \pm 0.01$
	DTT (4)	$7.1 \pm 0.2 \times 10^{-5}$	$0.5 \pm 0.02$	$5.7 \pm 0.4 \times 10^{-4}$	$0.3 \pm 0.03$	$1.3 \pm 0.2 \times 10^{-2}$	$0.1 \pm 0.01$
CCh/ $\alpha$ D97C/ $\alpha$ K25C (3)	Control (4)			$1.6 \pm 0.3 \times 10^{-4}$	$0.2 \pm 0.07$	$3.0 \pm 0.8 \times 10^{-3}$	$0.8 \pm 0.02$
	H <sub>2</sub> O <sub>2</sub> (4)			$1.4 \pm 0.7 \times 10^{-4}$	$0.1 \pm 0.04$	$2.4 \pm 0.2 \times 10^{-3}$	$0.9 \pm 0.03$
	DTT (4)			$2.2 \pm 0.2 \times 10^{-4}$	$0.4 \pm 0.03$	$2.3 \pm 0.2 \times 10^{-3}$	$0.6 \pm 0.03$
PIP/ $\alpha$ D97C/ $\alpha$ K125C (3)	Control (4)			$2.3 \pm 0.4 \times 10^{-4}$	$0.6 \pm 0.05$	$3.4 \pm 0.2 \times 10^{-3}$	$0.4 \pm 0.03$
	H <sub>2</sub> O <sub>2</sub> (4)			$2.1 \pm 0.2 \times 10^{-4}$	$0.4 \pm 0.08$	$2.7 \pm 0.4 \times 10^{-3}$	$0.6 \pm 0.10$
	DTT (4)			$2.5 \pm 0.7 \times 10^{-4}$	$0.4 \pm 0.03$	$2.6 \pm 0.3 \times 10^{-3}$	$0.6 \pm 0.03$
TMA/ $\alpha$ D97C/ $\alpha$ K125C (3)	Control (4)			$3.3 \pm 0.3 \times 10^{-4}$	$0.2 \pm 0.03$	$1.0 \pm 0.2 \times 10^{-3}$	$0.8 \pm 0.10$
	H <sub>2</sub> O <sub>2</sub> (4)			$1.2 \pm 0.3 \times 10^{-4}$	$0.4 \pm 0.02$	$1.1 \pm 0.1 \times 10^{-3}$	$0.6 \pm 0.05$
	DTT (4)			$2.2 \pm 0.2 \times 10^{-4}$	$0.4 \pm 0.07$	$9.9 \pm 0.1 \times 10^{-4}$	$0.6 \pm 0.07$

For each agonist/receptor/treatment combination, mean open durations and relative areas from a fit of the sum of exponentials were determined. Values listed are the mean  $\pm$  SD for the indicated number of patches.

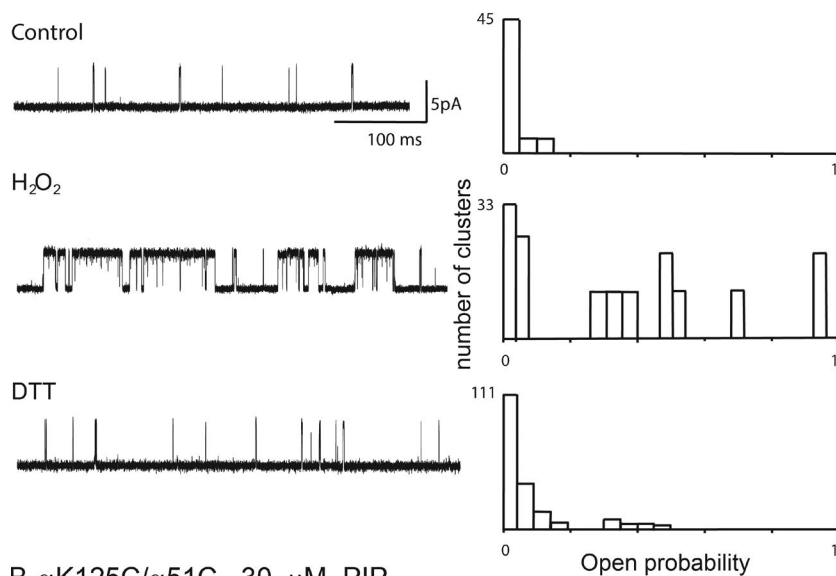
opening by PIP (Fig. S5 A and Table S3). Thus, cross-linking between  $\alpha$ T32C and  $\alpha$ Q59C, which like  $\alpha$ L109C and  $\alpha$ T117C stems from  $\beta$  strands that give rise to a shared  $\beta$  hairpin, suppressed channel opening by ACh but not that by other full or partial agonists.

As a control, we recorded single-channel currents elicited by either ACh or Cho from receptors with the single-cysteine substitutions  $\alpha$ T32C and  $\alpha$ Q59C. Unlike receptors containing the double-cysteine substitution, each single-mutant receptor opened robustly in the presence of either ACh or Cho (Fig. S5, E-H). Moreover, pretreatment of either single-mutant receptor with H<sub>2</sub>O<sub>2</sub> or subsequent treatment with DTT did not alter the mean open duration or cluster mean open probability for either of the agonists (Fig. S5, E-H; and Table S3). Thus, if H<sub>2</sub>O<sub>2</sub> chemically modified either of the single cysteine substitutions, any effects of the modification were not apparent in either ACh- or Cho-elicited single-channel currents.

### The pairs $\alpha$ Q59C/ $\alpha$ T117C and $\alpha$ T32C/ $\alpha$ N159C

The residues from each of these pairs stem from juxtaposed  $\beta$  strands at the complementary face of the subunit, but in contrast to the pairs just described, the  $\beta$  strands do not form a shared  $\beta$  hairpin; consequently, the residues of each pair are farther apart along the protein chain. In the presence of 30  $\mu$ M ACh, both mutant receptors exhibited a single exponential component of channel openings with mean durations of  $\sim$ 0.4 ms (Table S4), and the mean cluster open probability spanned from 0.1 to 0.8 (Fig. S6, A and G). Thus, the two mutant receptors showed only a mild loss of function compared with the wild-type receptor (Table 1). However, neither pretreatment with H<sub>2</sub>O<sub>2</sub> nor subsequent treatment with DTT affected channel opening by ACh (Fig. S6, A and G; and Table S4). Similarly, for SubCho, PIP, CCh, TMA, and Cho, neither pretreatment with H<sub>2</sub>O<sub>2</sub> nor subsequent treatment with DTT affected channel opening by any of these agonists (Fig. S6, B-F and H-L; and Table S4). In addition,

### A $\alpha$ K125C/ $\alpha$ 51C 300 nM ACh



### B $\alpha$ K125C/ $\alpha$ 51C 30 $\mu$ M PIP

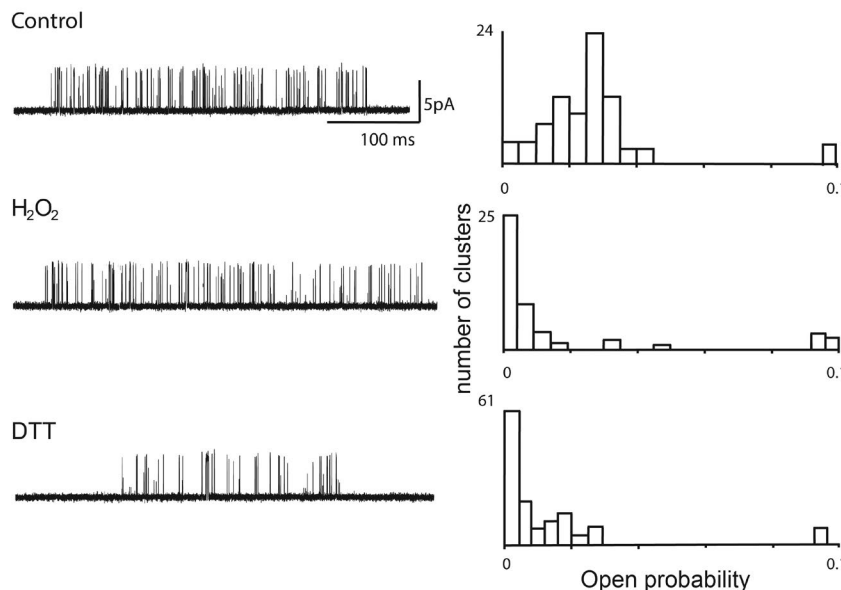


**Figure 7. Oxidative cross-linking of AChRs with cysteine substituted for  $\alpha$ T51 and  $\alpha$ K125 enhances channel opening by ACh but not other agonists. (A)** Single-channel currents from the  $\alpha$ D97C/ $\alpha$ K125C mutant receptor were recorded in the presence of ACh under control conditions (top trace), after pretreatment with H<sub>2</sub>O<sub>2</sub> (middle trace), or after successive treatment with H<sub>2</sub>O<sub>2</sub> and DTT (bottom trace); the middle and bottom traces were obtained from the same membrane patch. Individual clusters of channel openings, all from the same AChR channel, are shown at a bandwidth of 5 kHz (Gaussian response). To the right of each trace is a histogram of cluster open probability as in Fig. 2. **(B)** Same as in A, but with PIP as the agonist.

channel opening of receptors with the single-cysteine substitution  $\alpha$ N159C remained unaltered after pretreatment with either H<sub>2</sub>O<sub>2</sub> or DTT (Fig. S6, M and N; and Table S4), as also observed for  $\alpha$ Q59C (Fig. S5, E and F; and Table S4),  $\alpha$ T32C (Fig. S5, G and H; and Table S3), and  $\alpha$ T117C (Fig. S4, E and F; and Table S2). Thus, in contrast to residue pairs from  $\beta$  strands that give rise to a shared  $\beta$  hairpin, for pairs from noncontiguous  $\beta$  strands, neither oxidation nor reduction affected channel opening.

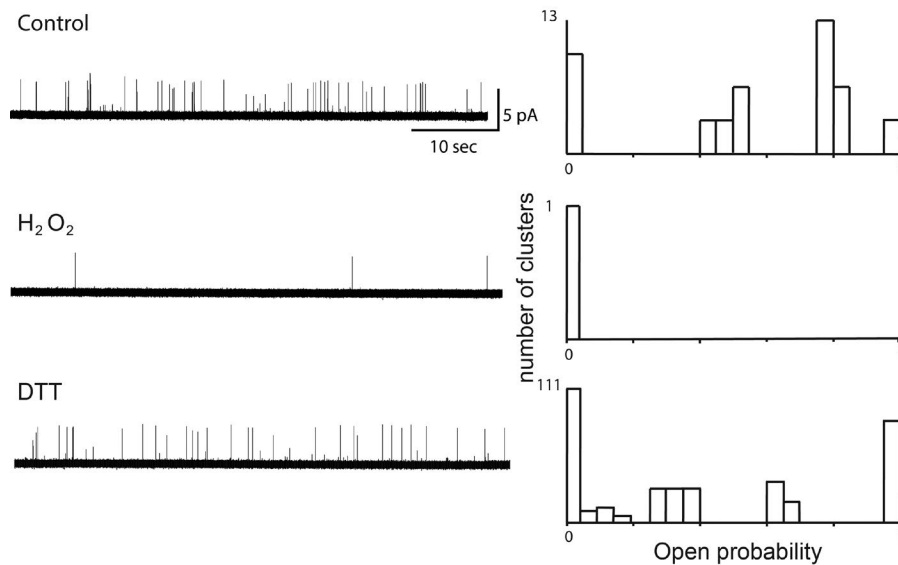
## Discussion

The results herein identify pairs of residues within the  $\alpha$  subunit of the muscle AChR that, when substituted with cysteine and subjected to oxidizing conditions, alter agonist-elicited channel opening. Moreover, whether oxidation alters channel opening depends on the particular agonist. For two residue pairs, the

changes upon oxidation depend on efficacy of the agonist, showing impaired activation by full but not partial agonists, whereas for three other pairs the changes are selective for the particular agonist. The results shed light on agonist-mediated structural changes at the level of individual residue positions and provide evidence that juxtaposed regions of the protein tertiary structure move relative to one another, suggesting that the  $\alpha$  subunits flex or twist during activation. The collective results show that different agonists elicit distinct structural changes in the course of opening the receptor channel and raise the possibility that intermediate agonist-bound receptor states may differ from one agonist to another.

The conclusion that different agonists elicit distinct structural changes linked to channel opening begins with the observation that a given agonist, say ACh, efficiently opens the channel of a receptor with a pair of substituted cysteines. However,

**A**  $\alpha$ L109C/ $\alpha$ T117C 30  $\mu$ M ACh



**B**  $\alpha$ L109C/ $\alpha$ T117C 30  $\mu$ M PIP

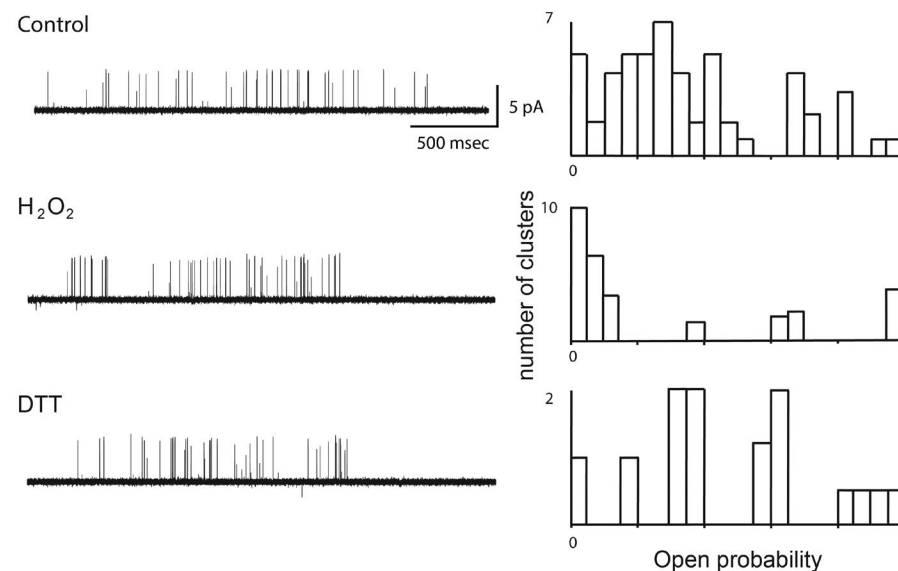


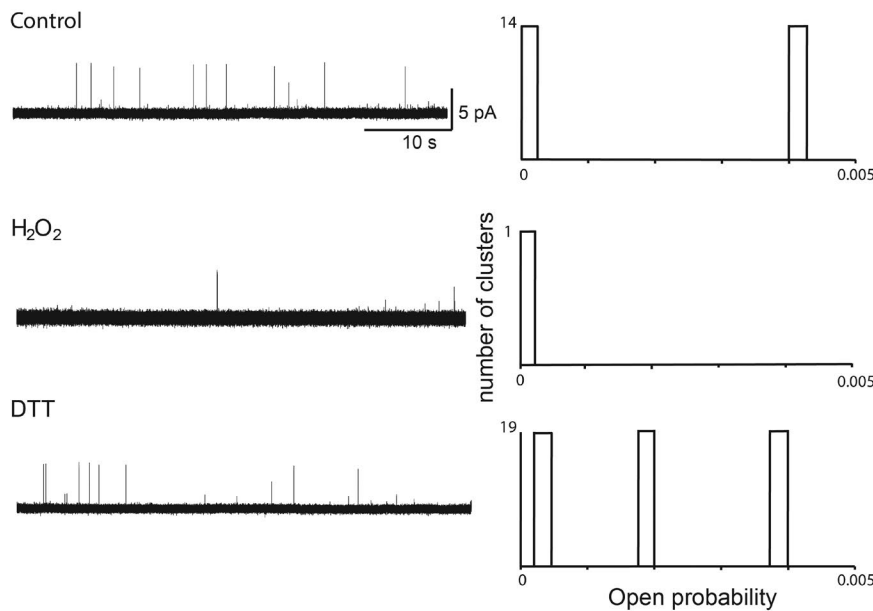
**Figure 8. Oxidative cross-linking of AChRs with cysteine substituted for  $\alpha$ L109 and  $\alpha$ T117 suppresses channel opening by ACh but not the partial agonist PIP. (A)** Single-channel currents from the  $\alpha$ L109/ $\alpha$ T117 mutant receptor were recorded in the presence of ACh under control conditions (top trace), after pretreatment with  $H_2O_2$  (middle trace), or after successive treatment with  $H_2O_2$  and DTT (bottom trace); the middle and bottom traces were obtained from the same membrane patch. Individual clusters of channel openings, all from the same AChR channel, are shown at a bandwidth of 5 kHz (Gaussian response). To the right of each trace is a histogram of cluster open probability as in Fig. 2. **(B)** Same as in A, but with PIP as the agonist.

pretreatment with  $H_2O_2$  markedly impairs opening of the channel, an effect reversed by DTT and not observed if cysteine is substituted for only one of the two residues of the pair. The loss of function after cross-linking means that the two residues need freedom to move, either relative to one another or dynamically, in order for the channel to open efficiently. In addition, the protein chains to which the two residues are attached may also need freedom to move. Furthermore, the residues and associated protein chains are either among the structures that transduce binding into channel opening, or they indirectly affect such structures. Conversely, because cross-linking does not affect channel opening by a partial agonist, the structures are either not among those that transduce binding of a partial agonist into channel opening, or they do not indirectly affect such structures. Regardless of whether the cysteine-substituted residues are part of the transduction pathway or coupled to such structures, the structural

changes linked to signal transduction are distinct between a full and a partial agonist. That pairs of cysteine substitutions in multiple locations show agonist dependence upon cross-linking strengthens the conclusion of distinct structural changes linked to channel opening.

Alternatively, the cysteine mutations themselves could potentially create multiple populations of resting state structures, for example, one activated by full agonists and another by partial agonists. Our results could be explained if cross-linking acted on one population but not the other. However, each population would have to be highly selective for the full versus partial agonist, otherwise before cross-linking, multiple classes of activation episodes should be evident for one or both types of agonists; none of the mutant/agonist combinations studied herein showed multiple classes of activation episodes. Thus, the possibility of multiple populations of resting state structures, though possible, seems unlikely.

**A**  $\alpha$ T32C/ $\alpha$ Q59C 30  $\mu$ M ACh



**B**  $\alpha$ T32C/ $\alpha$ Q59C 100 nM SubCho

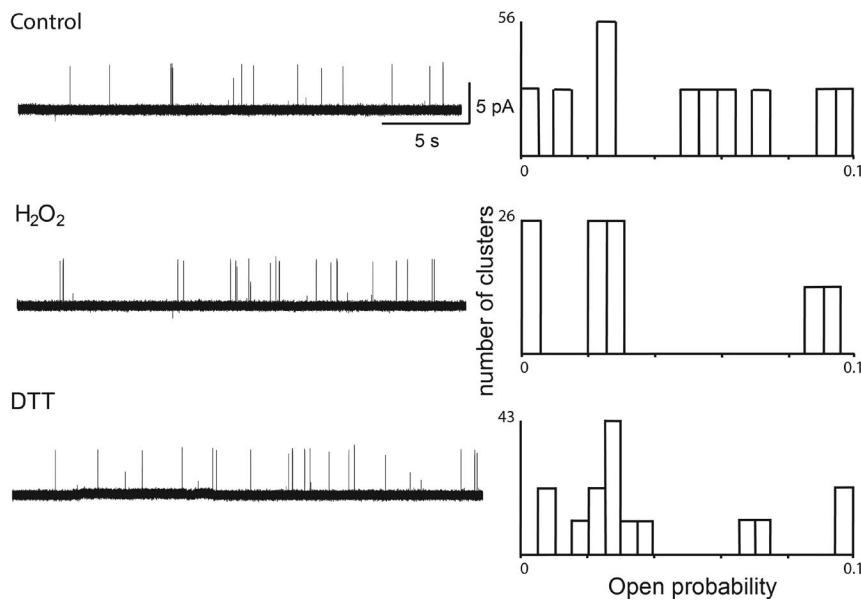


**Figure 9. Oxidative cross-linking of AChRs with cysteine substituted for  $\alpha$ T32 and  $\alpha$ Q59 selectively suppresses channel opening by ACh but not other agonists. (A)** Single-channel currents from the  $\alpha$ T32/ $\alpha$ Q59 mutant receptor were recorded in the presence of ACh under control conditions (top trace), after pretreatment with  $H_2O_2$  (middle trace), or after successive treatment with  $H_2O_2$  and DTT (bottom trace); the middle and bottom traces were obtained from the same membrane patch. Individual clusters of channel openings, all from the same AChR channel, are shown at a bandwidth of 5 kHz (Gaussian response). To the right of each trace is a histogram of cluster open probability as in Fig. 2. **(B)** Same as in A, but with SubCho as the agonist.

For the muscle AChR, differences in the channel opening step that follows agonist occupancy have traditionally been viewed as the origin of agonist efficacy (Del Castillo and Katz, 1957; Grosman et al., 2000). Within the framework of allosteric theory, a much greater affinity of ACh for the open relative to the resting closed state was thought to account for the ability of ACh to efficiently open the channel (Jackson, 1989). However, recent studies show that tighter binding of agonist to closed-state intermediates accounts for efficient channel opening by strong agonists, whereas weaker binding accounts for inefficient channel opening by partial agonists (Lape et al., 2008, 2009; Mukhtasimova et al., 2016). The results herein show that physically constraining

juxtaposed segments of the protein chain dramatically curtails the efficacy of some agonists without affecting that of others. The selectivity of these structural constraints for a particular agonist is not consistent with a mechanism in which all agonists transduce binding into channel gating via transition among a common set of closed state intermediates. Instead the findings suggest that, in transducing binding into channel gating, different agonists give rise to structurally distinct intermediate states.

Previous studies of ligand-gated receptor channels demonstrated that conformational changes within the ligand-binding pocket depend on the particular ligand. In the cysteine loop receptor surrogate ACh binding protein, crystal structures reveal that

loop C at the periphery of the binding site closes in upon the bound ligand (Celie et al., 2004; Hansen et al., 2005; Li et al., 2011). The extent of closure depended on the type of ligand, closing to the greatest extent with agonists and to a lesser extent with antagonists. Studies of AMPA-type glutamate receptors, which belong to a receptor family distinct from cystine loop receptors, showed that the clamshell structure of the ligand-binding domain closed to a greater extent when bound by a full than a partial agonist (Jin et al., 2003). Also in studies of the ligand-binding domain of the NMDA-type glutamate receptor, dynamic motions of the clamshell differed between strong and weak agonists and antagonists (Dolino et al., 2016). So far there is no structural evidence for cystine loop receptors that the conformation of loop C differs for agonists with differing efficacy.

Agonist-dependent conformational changes have also been observed in regions remote from the ligand-binding site. Studies of glycine receptors, in which a fluorescent probe was installed at the top of the M2  $\alpha$  helix that lines the pore, showed that full agonists elicited relatively large changes in fluorescence, whereas weak agonists elicited small changes (Pless et al., 2007). An advantage in those studies was that the modifications did not alter the relative efficacy of the agonists. Subsequent studies in which the fluorescent probe was placed at different locations within the extracellular domain also revealed changes in fluorescence that depended on efficacy of the agonist (Soh et al., 2017). However, in the fluorescently labeled receptors, the distinction between full and partial agonists was reduced or, for some locations, eliminated. Intriguingly, for some extracellular locations, a nominally weak agonist produced the largest fluorescence change despite eliciting the same maximal current flow as a nominally strong agonist, suggesting that either the extent or type of conformational change depended on the particular agonist. A possible interpretation of those studies is that all agonists produced the same structural change, but the extent to which the change occurred depended on the agonist. Alternatively, because the fluorescence changes were observed for a macroscopic population of receptors, all agonists may have produced identical conformational changes at the level of individual receptors, but the fraction of receptors that changed conformation may have depended on the agonist. In addition, macroscopic measurements could not distinguish whether gating modes with different channel open probability were present, or if present, whether the weighting of the different modes depended on the agonist.

An advantage of our experimental approach is that the receptors are studied at the single-channel level. Thus, our conclusions are based solely on the population of receptors that activate in response to agonist, and if an inactive population is present, it does not contribute to the measurements. In addition, the same receptors are monitored before and after structural modification, which is not possible in studies comparing wild-type and mutant receptors. Finally, after oxidative cross-linking, receptors within the same patch of membrane are assessed after reduction, so that each patch serves as its own control.

An inherent limitation of our studies is uncertainty of whether receptor function of the mutants is analogous to that of the wild-type receptor, although this is common to many studies of structure–function relationships. To counter this limitation,

we tested pairwise mutations in multiple locations of the extracellular domain, and for five of the seven pairs, we observed that functional changes upon cross-linking are agonist dependent. In addition, for several cysteine pairs, exemplified by the  $\alpha$ D97C/ $\alpha$ Y127C pair, the distinction between full and partial agonists is maintained. However, the gain-of-function pair  $\alpha$ D97C/ $\alpha$ K125C only partially maintains the distinction; Cho and PIP become strong agonists, whereas TMA remains a very weak agonist.

In light of these results, differences in agonist efficacy may be considered an example of biased signaling in which different ligands target the same orthosteric site but elicit different functional outcomes (Urban et al., 2007). Different agonists, owing to their different sizes and chemical compositions, may establish different interactions within the ligand binding site, lodging in different subregions of the site, establishing interactions of varying strength, or a combination of the two. Different docking poses have been observed for derivatives of the antagonist curare differing only in the number of methyl substitutions; the different derivatives bound in markedly different orientations and contacted different residues in AChR binding protein (Gao et al., 2003) and the human adult muscle AChR (Wang et al., 2003). Analogously, in G-protein–coupled receptors, different ligands have been shown to couple differentially between the G-protein and arrestin pathways, thus activating different second messengers and producing different physiological outcomes. In the case of  $\mu$ -opioid receptors, ligand bias toward the G-protein–coupled pathway enhances the therapeutic window for analgesia versus respiratory depression (Schmid et al., 2017), whereas for 5-HT<sub>2b</sub> receptors, ligand bias toward arrestin recruitment increases psychoactivity (Wacker et al., 2017).

Our results have implications for the design and interpretation of mutational analyses aimed to decipher structure–function relationships. Mutations within the orthosteric binding site could potentially alter the docking pose of an agonist and, as a consequence, alter structural changes linked to channel opening. Likewise, the effects of mutations at the binding site could depend on the structure of the agonist. Toward identifying inter-residue interactions that underpin protein function, mutant cycle analyses compare functional consequences of single and double mutations, and the overall coupling energy indicates whether the functional consequences of the mutations are additive or nonadditive. If different agonists elicit distinct structural changes, the overall coupling energy of a given mutant cycle could depend on the agonist used to monitor function (Mukhtasimova and Sine, 2013). Thus, in the design and interpretation of mutational analyses, the agonist itself becomes a crucial parameter.

The types of structural changes that accompany receptor function remain a topic of vigorous investigation. So far there is evidence for both rigid-body and twisting motions of the subunits (Cheng et al., 2007; Althoff et al., 2014; Kaczanowska et al., 2014; Du et al., 2015), but the relative importance of each type of motion is not established. Our observation that agonist occupancy prevents cross-linking between  $\alpha$ Y127C and  $\alpha$ D97C provides evidence that the signature cystine loop moves relative to the distal portion of loop A from the agonist binding site. In the resting state, these two structures are close enough to allow cross-linking, but when the agonist is bound, cross-linking is

prevented. Because the agonist was present at steady state before and during the application of oxidizing reagent, the increase in distance between  $\alpha$ Y127C and  $\alpha$ D97C likely corresponds to a change from the resting closed to the desensitized state. Moreover, such an interchain displacement is best explained by a twisting rather than a rigid-body motion. The findings also suggest that, at the complementary face of the subunit, antiparallel  $\beta$  strands flex upon transition to the open state, as cross-linking greatly attenuates channel opening. Alternatively, interchain cross-linking may restrict dynamic motions crucial for channel opening. Regardless of whether cross-linking restricts twisting or dynamic motions, our observation that the effects of cross-linking depend on the agonist shows that differences in agonist efficacy arise from distinct structural changes linked to channel opening.

## Acknowledgments

This work was supported by National Institutes of Health grant NS31744 to S.M. Sine.

The authors declare no competing financial interests.

Author contributions: N. Mukhtasimova conducted the experiments and analyzed the data. S.M. Sine wrote the manuscript. Both authors discussed the results and commented on the manuscript.

Merritt C. Maduke served as editor.

Submitted: 16 August 2017

Revised: 8 January 2018

Accepted: 12 March 2018

## References

- Althoff, T., R.E. Hibbs, S. Banerjee, and E. Gouaux. 2014. X-ray structures of GluCl in apo states reveal a gating mechanism of Cys-loop receptors. *Nature*. 512:333–337. <https://doi.org/10.1038/nature13669>
- Brejč, K., W.J. van Dijk, R.V. Klaassen, M. Schuurmans, J. van Der Oost, A.B. Smit, and T.K. Sixma. 2001. Crystal structure of an ACh-binding protein reveals the ligand-binding domain of nicotinic receptors. *Nature*. 411:269–276. <https://doi.org/10.1038/35077011>
- Celie, P.H., S.E. van Rossum-Fikkert, W.J. van Dijk, K. Brejč, A.B. Smit, and T.K. Sixma. 2004. Nicotine and carbamylcholine binding to nicotinic acetylcholine receptors as studied in AChBP crystal structures. *Neuron*. 41:907–914. [https://doi.org/10.1016/S0896-6273\(04\)00115-1](https://doi.org/10.1016/S0896-6273(04)00115-1)
- Cheng, X., I. Ivanov, H. Wang, S.M. Sine, and J.A. McCammon. 2007. Nanosecond-timescale conformational dynamics of the human  $\alpha$ 7 nicotinic acetylcholine receptor. *Biophys. J.* 93:2622–2634. <https://doi.org/10.1529/biophysj.107.109843>
- Colquhoun, D. 1998. Binding, gating, affinity and efficacy: The interpretation of structure-activity relationships for agonists and of the effects of mutating receptors. *Br. J. Pharmacol.* 125:924–947. <https://doi.org/10.1038/sj.bjp.0702164>
- Colquhoun, D., and F. Sigworth. 1983. Fitting and statistical analysis of single channel records. *In* Single Channel Recording. B. Sakmann and E. Neher, editors. Plenum Publishing Corp., New York. 191–264.
- Del Castillo, J., and B. Katz. 1957. Interaction at end-plate receptors between different choline derivatives. *Proc. R. Soc. Lond. B Biol. Sci.* 146:369–381. <https://doi.org/10.1098/rspb.1957.0018>
- Dellisanti, C.D., Y. Yao, J.C. Stroud, Z.Z. Wang, and L. Chen. 2007. Crystal structure of the extracellular domain of nAChR  $\alpha$ 1 bound to  $\alpha$ -bungarotoxin at 1.94 Å resolution. *Nat. Neurosci.* 10:953–962. <https://doi.org/10.1038/nn1942>
- Dolino, D.M., S. Rezaei Adariani, S.A. Shaikh, V. Jayaraman, and H. Sanabria. 2016. Conformational selection and submillisecond dynamics of the ligand-binding domain of the N-methyl-D-aspartate receptor. *J. Biol. Chem.* 291:16175–16185. <https://doi.org/10.1074/jbc.M116.721274>
- Du, J., W. Lü, S. Wu, Y. Cheng, and E. Gouaux. 2015. Glycine receptor mechanism elucidated by electron cryo-microscopy. *Nature*. 526:224–229. <https://doi.org/10.1038/nature14853>
- Gao, F., N. Bern, A. Little, H.-L. Wang, S.B. Hansen, T.T. Talley, P. Taylor, and S.M. Sine. 2003. Curariform antagonists bind in different orientations to acetylcholine-binding protein. *J. Biol. Chem.* 278:23020–23026. <https://doi.org/10.1074/jbc.M301151200>
- Grosman, C., M. Zhou, and A. Auerbach. 2000. Mapping the conformational wave of acetylcholine receptor channel gating. *Nature*. 403:773–776. <https://doi.org/10.1038/35001586>
- Hansen, S.B., G. Sulzenbacher, T. Huxford, P. Marchot, P. Taylor, and Y. Bourne. 2005. Structures of Aplysia AChBP complexes with nicotinic agonists and antagonists reveal distinctive binding interfaces and conformations. *EMBO J.* 24:3635–3646. <https://doi.org/10.1038/sj.emboj.7600828>
- Hassaine, G., C. Deluz, L. Grasso, R. Wyss, M.B. Tol, R. Hovius, A. Graff, H. Stahlberg, T. Tomizaki, A. Desmyter, et al. 2014. X-ray structure of the mouse serotonin 5-HT<sub>3</sub> receptor. *Nature*. 512:276–281. <https://doi.org/10.1038/nature13552>
- Jackson, M.B. 1989. Perfection of a synaptic receptor: Kinetics and energetics of the acetylcholine receptor. *Proc. Natl. Acad. Sci. USA.* 86:2199–2203. <https://doi.org/10.1073/pnas.86.7.2199>
- Jin, R., T.G. Banke, M.L. Mayer, S.F. Traynelis, and E. Gouaux. 2003. Structural basis for partial agonist action at ionotropic glutamate receptors. *Nat. Neurosci.* 6:803–810. <https://doi.org/10.1038/nn1091>
- Kaczanowska, K., M. Harel, Z. Radić, J.P. Changeux, M.G. Finn, and P. Taylor. 2014. Structural basis for cooperative interactions of substituted 2-aminopyrimidines with the acetylcholine binding protein. *Proc. Natl. Acad. Sci. USA.* 111:10749–10754. <https://doi.org/10.1073/pnas.1410992111>
- Lape, R., D. Colquhoun, and L.G. Sivilotti. 2008. On the nature of partial agonism in the nicotinic receptor superfamily. *Nature*. 454:722–727. <https://doi.org/10.1038/nature07139>
- Lape, R., P. Krashia, D. Colquhoun, and L.G. Sivilotti. 2009. Agonist and blocking actions of choline and tetramethylammonium on human muscle acetylcholine receptors. *J. Physiol.* 587:5045–5072. <https://doi.org/10.1113/jphysiol.2009.176305>
- Lee, B.S., R.B. Gunn, and R.R. Kopito. 1991. Functional differences among nonerythroid anion exchangers expressed in a transfected human cell line. *J. Biol. Chem.* 266:11448–11454.
- Li, S., S. Huang, N. Bren, K. Noridomi, C.D. Dellisanti, S.M. Sine, and L. Chen. 2011. Ligand-binding domain of an  $\alpha$ 7-nicotinic receptor chimera and its complex with agonist. *Nat. Neurosci.* 14:1253–1259. <https://doi.org/10.1038/nn.2908>
- Liu, Y., and J.P. Dilger. 1991. Opening rate of acetylcholine receptor channels. *Biophys. J.* 60:424–432. [https://doi.org/10.1016/S0006-3495\(91\)82068-9](https://doi.org/10.1016/S0006-3495(91)82068-9)
- Liu, Y., and J.P. Dilger. 1993. Decamethonium is a partial agonist at the nicotinic acetylcholine receptor. *Synapse*. 13:57–62. <https://doi.org/10.1002/syn.890130108>
- Maconochie, D.J., and J.H. Steinbach. 1998. The channel opening rate of adult- and fetal-type mouse muscle nicotinic receptors activated by acetylcholine. *J. Physiol.* 506:53–72. <https://doi.org/10.1111/j.1469-7793.1998.053bx.x>
- Morales-Perez, C.L., C.M. Novello, and R.E. Hibbs. 2016. X-ray structure of the human  $\alpha$ 4 $\beta$ 2 nicotinic receptor. *Nature*. 538:411–415. <https://doi.org/10.1038/nature19785>
- Mukhtasimova, N., and S.M. Sine. 2007. An intersubunit trigger of channel gating in the muscle nicotinic receptor. *J. Neurosci.* 27:4110–4119. <https://doi.org/10.1523/JNEUROSCI.0025-07.2007>
- Mukhtasimova, N., and S.M. Sine. 2013. Nicotinic receptor transduction zone: Invariant arginine couples to multiple electron-rich residues. *Biophys. J.* 104:355–367. <https://doi.org/10.1016/j.bpj.2012.12.013>
- Mukhtasimova, N., W.Y. Lee, H.-L. Wang, and S.M. Sine. 2009. Detection and trapping of intermediate states priming nicotinic receptor channel opening. *Nature*. 459:451–454. <https://doi.org/10.1038/nature07923>
- Mukhtasimova, N., C.J. daCosta, and S.M. Sine. 2016. Improved resolution of single channel dwell times reveals mechanisms of binding, priming, and gating in muscle AChR. *J. Gen. Physiol.* 148:43–63. <https://doi.org/10.1085/jgp.201611584>
- Pear, W.S., G.P. Nolan, M.L. Scott, and D. Baltimore. 1993. Production of high-titer helper-free retroviruses by transient transfection. *Proc.*

- Natl. Acad. Sci. USA. 90:8392–8396. <https://doi.org/10.1073/pnas.90.18.8392>
- Pless, S.A., M.I. Dibas, H.A. Lester, and J.W. Lynch. 2007. Conformational variability of the glycine receptor M2 domain in response to activation by different agonists. *J. Biol. Chem.* 282:36057–36067. <https://doi.org/10.1074/jbc.M706468200>
- Sakmann, B., J. Patlak, and E. Neher. 1980. Single acetylcholine-activated channels show burst-kinetics in presence of desensitizing concentrations of agonist. *Nature.* 286:71–73. <https://doi.org/10.1038/286071a0>
- Schmid, C.L., N.M. Kennedy, N.C. Ross, K.M. Lovell, Z. Yue, J. Morgenweck, M.D. Cameron, T.D. Bannister, and L.M. Bohn. 2017. Bias Factor and Therapeutic Window Correlate to Predict Safer Opioid Analgesics. *Cell.* 171:1165–1175.e13. <https://doi.org/10.1016/j.cell.2017.10.035>
- Sigworth, F.J., and S.M. Sine. 1987. Data transformations for improved display and fitting of single-channel dwell time histograms. *Biophys. J.* 52:1047–1054. [https://doi.org/10.1016/S0006-3495\(87\)83298-8](https://doi.org/10.1016/S0006-3495(87)83298-8)
- Sine, S.M., T. Claudio, and F.J. Sigworth. 1990. Activation of Torpedo acetylcholine receptors expressed in mouse fibroblasts. Single channel current kinetics reveal distinct agonist binding affinities. *J. Gen. Physiol.* 96:395–437. <https://doi.org/10.1085/jgp.96.2.395>
- Soh, M.S., A. Estrada-Mondragon, N. Durisic, A. Keramidas, and J.W. Lynch. 2017. Probing the structural mechanism of partial agonism in glycine receptors using the fluorescent artificial amino acid, ANAP. *ACS Chem. Biol.* 12:805–813. <https://doi.org/10.1021/acscchembio.6b00926>
- Unwin, N. 2005. Refined structure of the nicotinic acetylcholine receptor at 4Å resolution. *J. Mol. Biol.* 346:967–989. <https://doi.org/10.1016/j.jmb.2004.12.031>
- Urban, J.D., W.P. Clarke, M. von Zastrow, D.E. Nichols, B. Kobilka, H. Weinstein, J.A. Javitch, B.L. Roth, A. Christopoulos, P.M. Sexton, et al. 2007. Functional selectivity and classical concepts of quantitative pharmacology. *J. Pharmacol. Exp. Ther.* 320:1–13. <https://doi.org/10.1124/jpet.106.104463>
- Wacker, D., S. Wang, J.D. McCorvy, R.M. Betz, A.J. Venkatakrishnan, A. Levit, K. Lansu, Z.L. Schools, T. Che, D.E. Nichols, et al. 2017. Crystal structure of an LSD-bound human serotonin receptor. *Cell.* 168:377–389.
- Wang, H.-L., F. Gao, N. Bren, and S.M. Sine. 2003. Curariform antagonists bind in different orientations to the nicotinic receptor ligand binding domain. *J. Biol. Chem.* 278:32284–32291.